

AD-A015 052

TIME-DOMAIN WIENER ADAPTIVE BEAMFORMING WITH DISTRIBUTED
SIGNAL MODELS

Thomas E. Barnard

Texas Instruments, Incorporated

Prepared for:

Advanced Research Projects Agency
Air Force Technical Applications Center

16 June 1975

DISTRIBUTED BY:

NTIS

National Technical Information Service
U. S. DEPARTMENT OF COMMERCE



276103

APPROVED FOR PUBLIC RELEASE, DISTRIBUTION UNLIMITED

ALEX(01)-TR-75-03

ADA 015052

**TIME-DOMAIN WIENER ADAPTIVE BEAMFORMING
WITH DISTRIBUTED SIGNAL MODELS**

TECHNICAL REPORT NO. 3

VELA NETWORK EVALUATION AND AUTOMATIC PROCESSING RESEARCH

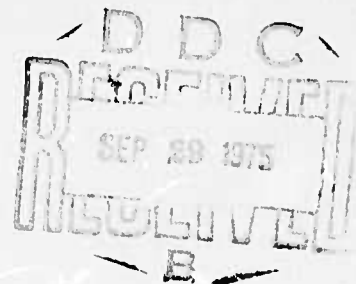
Prepared by
Thomas E. Barnard

TEXAS INSTRUMENTS INCORPORATED
Equipment Group
Post Office Box 6015
Dallas, Texas 75222

Prepared for
AIR FORCE TECHNICAL APPLICATIONS CENTER
AFTAC Project No. VELA T/5705/B/ETR
Alexandria, Virginia 22314

Sponsored by
ADVANCED RESEARCH PROJECTS AGENCY
Nuclear Monitoring Research Office
ARPA Program Code No. 4F10
ARPA Order No. 2551

16 June 1975



Acknowledgment: This research was supported by the Advanced Research Projects Agency, Nuclear Monitoring Research Office, under Project VELA-UNIFORM, and accomplished under the technical direction of the Air Force Technical Applications Center under Contract No. F08606-75-C-0029.

Reproduced by
NATIONAL TECHNICAL
INFORMATION SERVICE
US Department of Commerce
Springfield, VA. 22151

Equipment Group



**TIME-DOMAIN WIENER ADAPTIVE BEAMFORMING
WITH DISTRIBUTED SIGNAL MODELS**

TECHNICAL REPORT NO. 3

VELA NETWORK EVALUATION AND AUTOMATIC PROCESSING RESEARCH

Prepared by
Thomas E. Barnard

TEXAS INSTRUMENTS INCORPORATED
Equipment Group
Post Office Box 6015
Dallas, Texas 75222

Prepared for
AIR FORCE TECHNICAL APPLICATIONS CENTER
AFTAC Project No. VELA T/5705/B/ETR
Alexandria, Virginia 22314

Sponsored by
ADVANCED RESEARCH PROJECTS AGENCY
Nuclear Monitoring Research Office
ARPA Program Code No. 4F10
ARPA Order No. 2551

16 June 1975

Acknowledgment: This research was supported by the Advanced Research Projects Agency, Nuclear Monitoring Research Office, under Project VELA-UNIFORM, and accomplished under the technical direction of the Air Force Technical Applications Center under Contract No. F08606-75-C-0029.

UNCLASSIFIED

SECURITY CLASSIFICATION OF THIS PAGE (When Data Entered)

REPORT DOCUMENTATION PAGE		READ INSTRUCTIONS BEFORE COMPLETING FORM
1. REPORT NUMBER	2. GOVT ACCESSION NO.	3. RECIPIENT'S CATALOG NUMBER
4. TITLE (and Subtitle) TIME-DOMAIN WIENER ADAPTIVE BEAM-FORMING WITH DISTRIBUTED SIGNAL MODELS		5. TYPE OF REPORT & PERIOD COVERED Technical
7. AUTHOR(s) Thomas E. Barnard		6. PERFORMING ORG. REPORT NUMBER ALEX(01)-TR-75-03
9. PERFORMING ORGANIZATION NAME AND ADDRESS Texas Instruments Incorporated Equipment Group Dallas, Texas 75222		8. CONTRACT OR GRANT NUMBER(s) F08606-75-C-0029
11. CONTROLLING OFFICE NAME AND ADDRESS Advanced Research Projects Agency Nuclear Monitoring Research Office Arlington, Virginia 22209		10. PROGRAM ELEMENT PROJECT, TASK AREA & WORK UNIT NUMBERS VELA T/5705/B/ETR
14. MONITORING AGENCY NAME & ADDRESS (if different from Controlling Office) Air Force Technical Applications Center VELA Seismological Center Alexandria, Virginia 22314		12. REPORT DATE 16 June 1975
15. DISTRIBUTION STATEMENT (of this Report) APPROVED FOR PUBLIC RELEASE, DISTRIBUTION UNLIMITED		13. NUMBER OF PAGES 66
17. DISTRIBUTION STATEMENT (of the abstract entered in Block 20, if different from Report)		15. SECURITY CLASS. (of this report) UNCLASSIFIED
19. SUPPLEMENTARY NOTES ARPA Order No. 2551		16. DECLASSIFICATION/DOWNGRADING SCHEDULE
19. KEY WORDS (Continue on reverse side if necessary and identify by block number) Seismology Distributed signal models Adaptive beamforming Maximum likelihood beamforming Wiener multichannel filtering Crosscorrelation function		
20. ABSTRACT (Continue on reverse side if necessary and identify by block number) This report is a mathematical study of time-domain Wiener adaptive multichannel filtering using distributed signal models. It presents derivations for two Wiener adaptive algorithms and describes the basic technique for implementing a Wiener adaptive processor with directionally distributed signal models. In order to obtain the signal-model crosscorrelation functions needed		

UNCLASSIFIED

SECURITY CLASSIFICATION OF THIS PAGE (When Data Entered)

20. Continued

in the Wiener adaptive algorithms, the probability density function $p(\tau)$ for the time delay between a reference sensor and the individual channels must be specified. Analytic derivations of this function are presented for inverse velocity space models, distributed ring models, and velocity-azimuth space models. These derivations are of interest in their own right: they are useful in specifying two-channel crosscorrelation functions for various directional energy distributions.

ia

UNCLASSIFIED

SECURITY CLASSIFICATION OF THIS PAGE (When Data Entered)

ACKNOWLEDGMENT

Mrs. Bonnie C. Taylor typed virtually all of the text. Both Mrs. Taylor and Mrs. Cherylann Saunders prepared the figures for this report.

ABSTRACT

This report is a mathematical study of time-domain Wiener adaptive multichannel filtering using distributed signal models. It presents derivations for two Wiener adaptive algorithms and describes the basic technique for implementing a Wiener adaptive processor with directionally distributed signal models.

In order to obtain the signal-model crosscorrelation functions needed in the Wiener adaptive algorithms, the probability density function $p(\tau)$ for the time delay between a reference sensor and the individual channels must be specified. Analytic derivations of this function are presented for inverse velocity space models, distributed ring models, and velocity-azimuth space models. These derivations are of interest in their own right: they are useful in specifying two-channel crosscorrelation functions for various directional energy distributions.

Neither the Advanced Research Projects Agency nor the Air Force Technical Applications Center will be responsible for information contained herein which has been supplied by other organizations or contractors, and this document is subject to later revision as may be necessary. The views and conclusions presented are those of the authors and should not be interpreted as necessarily representing the official policies, either expressed or implied, of the Advanced Research Projects Agency, the Air Force Technical Applications Center, or the US Government.

TABLE OF CONTENTS

SECTION	TITLE	PAGE
	ACKNOWLEDGMENT	iii
	ABSTRACT	iv
I.	INTRODUCTION	I-1
II.	IMPLEMENTATION OF WIENER ADAPTIVE FILTERING WITH DISTRIBUTED SIGNAL MODELS	II-1
	A. DISCUSSION	II-1
	B. DERIVATION OF WIENER ADAPTIVE FILTERING ALGORITHMS	II-3
	C. ESTIMATION OF THE CROSS- CORRELATION VECTOR	II-8
III.	INVERSE VELOCITY SPACE MODELS	III-1
	A. BASIC APPROACH	III-1
	B. DISK MODEL	III-3
	C. ANNULAR MODEL	III-4
	D. SECTOR -OF- ANNULUS MODEL	III-6
IV.	DISTRIBUTION RING MODEL	IV-1
V.	VELOCITY -AZIMUTH SPACE MODELS	V-1
	A. BASIC APPROACH	V-1
	B. UNIFORM RECTANGULAR DISTRIBUTION	V-4
	C. TAPERED-VELOCITY UNIFORM AZIMUTH DISTRIBUTION	V-11
VI.	SUMMARY	VI-1
VII.	REFERENCE	VII-1

LIST OF FIGURES

FIGURE	TITLE	PAGE
II-1	DIAGRAMMATIC REPRESENTATION OF THE FACTORS DETERMINING THE TIME LAG OF THE SIGNAL BETWEEN TWO SENSORS	II-9
III-1	THE BASIC INVERSE VELOCITY SPACE MODEL	III-2
III-2	TIME-LAG PROBABILITY DENSITY FUNCTION FOR THE INVERSE VELOCITY SPACE DISK MODEL	III-5
III-3	TIME-LAG PROBABILITY DENSITY FUNCTION FOR THE INVERSE VELOCITY SPACE ANNULAR MODEL AT NINE VALUES OF V_{\min}/V_{\max}	III-7
III-4	PROCEDURE FOR MAPPING ANGLES BETWEEN θ_{\min} AND θ_{\max} ONTO FIRST AND SECOND QUADRANTS	III-8
III-5	THE TWO FIRST-QUADRANT POSSIBILITIES AFFECTING THE FORMULAS FOR THE TIME-LAG PROBABILITY DENSITY FUNCTION	III-10
III-6	TIME-LAG PROBABILITY DENSITY FUNCTION FOR THE INVERSE VELOCITY SPACE SECTOR-OF-ANNULUS MODEL AT $V_{\min}/V_{\max} = 0.1$ FOR VARIOUS 30° SECTORS	III-13
III-7	TIME-LAG PROBABILITY DENSITY FUNCTION FOR THE INVERSE VELOCITY SPACE SECTOR-OF-ANNULUS MODEL AT $V_{\min}/V_{\max} = 0.9$ FOR VARIOUS 30° SECTORS	III-14
IV-1	TRANSFORMATION FROM VELOCITY-AZIMUTH SPACE TO DELAY-AZIMUTH SPACE FOR DISTRIBUTED RING MODEL	IV-2
IV-2	TIME-LAG PROBABILITY DENSITY FUNCTION FOR THE DISTRIBUTED RING MODEL WITH A UNIFORM DISTRIBUTION OVER VARIOUS 30° SECTORS	IV-5

LIST OF FIGURES
(continued)

FIGURE	TITLE	PAGE
IV-3	TIME-LAG PROBABILITY DENSITY FUNCTION FOR THE DISTRIBUTED RING MODEL WITH INCOMING ENERGY EQUALLY LIKELY AT ALL AZIMUTHS	IV-6
IV-4	TIME-LAG PROBABILITY DENSITY FUNCTION FOR THE DISTRIBUTED RING MODEL WITH A NORMAL DISTRIBUTION ($\sigma = 15^\circ$) PEAKING AT VARIOUS ANGLES	IV-7
V-1	TRANSFORMATION FROM (v, θ) SPACE TO (τ, θ) SPACE	V-2
V-2	TIME-LAG PROBABILITY DENSITY FUNCTION FOR THE UNIFORM RECTANGULAR VELOCITY-AZIMUTH MODEL AT $v_{\min}/v_{\max} = 0.1$ FOR VARIOUS 30° SECTORS	V-9
V-3	TIME-LAG PROBABILITY DENSITY FUNCTION FOR THE UNIFORM RECTANGULAR VELOCITY-AZIMUTH MODEL AT $v_{\min}/v_{\max} = 0.9$ FOR VARIOUS 30° SECTORS	V-10
V-4	TAPERED VELOCITY PROBABILITY DENSITY FUNCTION	V-13
V-5	TIME-LAG PROBABILITY DENSITY FUNCTION FOR THE TAPERED-VELOCITY UNIFORM-AZIMUTH MODEL AT $v_{\min}/v_{\max} = 0.1$ FOR VARIOUS 30° SECTORS	V-19
V-6	TIME-LAG PROBABILITY DENSITY FUNCTION FOR THE TAPERED-VELOCITY UNIFORM-AZIMUTH MODEL AT $v_{\min}/v_{\max} = 0.9$ FOR VARIOUS 30° SECTORS	V-20

SECTION I INTRODUCTION

This report presents the results of a mathematic study directed toward implementation of Wiener adaptive multichannel filtering with distributed signal models.

Section II discusses the reasons for using this form of Wiener filtering, derives both an unconstrained Wiener adaptive algorithm and a Wiener adaptive algorithm subject to the same unity-response constraints as specified in the maximum likelihood adaptive algorithm, and describes a technique for modeling the signal crosscorrelation functions needed in the Wiener adaptive algorithms.

Sections III through V give analytic derivations for the time-lag probability density function corresponding to specific distributed signal models. The time-lag probability density function $p(\tau)$ for the time delay between the reference sensor and the individual channels is necessary in order to obtain the signal-model crosscorrelation functions in the Wiener adaptive algorithms. Section III features inverse velocity space models, Section IV distributed ring models, and Section V velocity-azimuth space models.

Section VI summarizes the results of this mathematical study.

SECTION II
 IMPLEMENTATION OF WIENER ADAPTIVE FILTERING
 WITH DISTRIBUTED SIGNAL MODELS

A. DISCUSSION

A previous adaptive-filtering study (Barnard and O'Brien, 1974) employed a maximum likelihood adaptive algorithm where the adaptive filter output $y(t)$ was formed using the equation

$$y(t) = X^T A$$

and the adaptive filter vector A was updated according to the equation

$$A(t+\Delta t) - A(t) = 2\mu(t) X^T A(\bar{X}-X) = 2\mu(t) y(t)(\bar{X}-X),$$

where the filter weight vector A , the data vector X , and the beamsteer output vector \bar{X} are, respectively,

$$A = \begin{bmatrix} a_1(-N) \\ \vdots \\ a_M(-N) \\ \vdots \\ a_1(0) \\ \vdots \\ a_M(0) \\ \vdots \\ a_1(N) \\ \vdots \\ a_M(N) \end{bmatrix}, \quad X = \begin{bmatrix} x_1(t+N) \\ \vdots \\ x_M(t+N) \\ \vdots \\ x_1(t) \\ \vdots \\ x_M(t) \\ \vdots \\ x_1(t-N) \\ \vdots \\ x_M(t-N) \end{bmatrix}, \quad \text{and } \bar{X} = \begin{bmatrix} \bar{x}(t+N) \\ \vdots \\ \bar{x}(t+N) \\ \vdots \\ \bar{x}(t) \\ \vdots \\ \bar{x}(t) \\ \vdots \\ \bar{x}(t-N) \\ \vdots \\ \bar{x}(t-N) \end{bmatrix}.$$

$\mu(t)$ is a scalar quantity controlling the convergence rate. The superscript T denotes vector transpose. M is the number of channels, and $2N+1$ is the total length of the adaptive filter in points. After time-shifting the input channels to align energy from the specified look direction, the quantities $x_i(t-j)$ inside the data vector X are the values for channel i at time $t-j\Delta t$, where Δt is the sampling interval. Inside each subvector of the beamsteer output vector \bar{X} , all vector components are identical and equal to the beamsteer output

$$\bar{x}(t-j) = \frac{1}{M} \sum_{i=1}^M x_i(t-j)$$

at time $t - j\Delta t$.

When operating against background noise from the Alaska Long Period Array (ALPA), the maximum likelihood adaptive algorithm (as implemented in the study mentioned) functioned well and produced 6 dB signal-to-noise-ratio improvements with suitably chosen operating parameters. In interfering-event simulations using ALPA data, the same algorithm produced significant detection gains but distorted the on-azimuth signal waveform considerably. The distortion was principally a result of the maximum likelihood design goal (minimization of the filter output power $y^2(t)$ subject to unity-response constraints in the beam look direction). In conformity with this design goal, the adaptive processor attempted to create from the data sample containing the off-azimuth interfering event a filter output 180° out of phase with the data sample containing the on-azimuth event and was partially successful in producing mutual cancellation of the two events. A possible remedy for this problem is a Wiener adaptive filtering algorithm, where the design goal is to minimize the mean square difference between the adaptive filter output and the on-azimuth signal. Conceivably, such an algorithm might even provide substantial detection improvement over the maximum likelihood algorithm actually employed.

The subject of this section is the basic technique for implementing a Wiener adaptive processor using distributed signal models. Discussion of specific distributed signal models is confined to later sections of this report. Subsection B in this section presents derivations for both an unconstrained Wiener adaptive algorithm and a Wiener adaptive algorithm subject to the same unity-response constraints in the look direction as specified in the maximum likelihood adaptive algorithm. Both of the derived algorithms require some method for estimating the crosscorrelation functions between the signal and the channels entering the adaptive beamformer. Subsection C describes a technique for modeling the crosscorrelation functions needed in the Wiener adaptive algorithm.

B. DERIVATION OF WIENER ADAPTIVE FILTERING ALGORITHMS

In the case of the unconstrained Wiener adaptive filtering algorithm, the derivation is relatively straightforward. The error $\epsilon(t)$ in estimating the signal $s(t)$ is $\epsilon(t) = s(t) - A^T X$ and the mean square error is

$$\begin{aligned} \overline{\epsilon^2(t)} &= \overline{[s(t) - A^T X][s(t) - X^T A]} \\ &= \overline{s^2(t)} - 2A^T \overline{Xs(t)} + A^T \overline{XX^T} A. \end{aligned}$$

When the Widrow approximation $\overline{XX^T} \approx XX^T$ is used in this expression, the gradient of the mean square error is

$$\nabla \left[\overline{\epsilon^2(t)} \right] = 2XX^T A - 2V,$$

where

$$V = \overline{Xs(t)} =$$

$$\begin{bmatrix} x_1(t+N) s(t) \\ \vdots \\ x_M(t+N) s(t) \\ \vdots \\ x_1(t) s(t) \\ \vdots \\ x_M(t) s(t) \\ \vdots \\ x_1(t-N) s(t) \\ \vdots \\ x_M(t-N) s(t) \end{bmatrix}$$

The method of steepest descent specifies that the adaptive filter vector moves in the direction opposite to that of the gradient:

$$A(t + \Delta t) - A(t) = 2\mu(t) [V - XX^T A] = 2\mu(t) [V - y(t)X]$$

In the case of the Wiener adaptive algorithm with unity-response constraints in the look direction, the constraints are expressed in the matrix equation

$$\begin{bmatrix} \begin{bmatrix} 1 & \dots & 1 \end{bmatrix} & \begin{bmatrix} 0 & \dots & 0 \end{bmatrix} & \dots & \begin{bmatrix} 0 & \dots & 0 \end{bmatrix} \\ \begin{bmatrix} 0 & \dots & 0 \end{bmatrix} & \begin{bmatrix} 1 & \dots & 1 \end{bmatrix} & \begin{bmatrix} 0 & \dots & 0 \end{bmatrix} & \dots & \begin{bmatrix} 0 & \dots & 0 \end{bmatrix} \\ \vdots & \vdots & \vdots & \vdots & \vdots \\ \begin{bmatrix} 0 & \dots & 0 \end{bmatrix} & \dots & \begin{bmatrix} 0 & \dots & 0 \end{bmatrix} & \begin{bmatrix} 1 & \dots & 1 \end{bmatrix} & \begin{bmatrix} 0 & \dots & 0 \end{bmatrix} \\ \begin{bmatrix} 0 & \dots & 0 \end{bmatrix} & \dots & \begin{bmatrix} 0 & \dots & 0 \end{bmatrix} & \begin{bmatrix} 0 & \dots & 0 \end{bmatrix} & \begin{bmatrix} 1 & \dots & 1 \end{bmatrix} \end{bmatrix} \begin{bmatrix} A \end{bmatrix} = \begin{bmatrix} D \end{bmatrix}$$

where each of the row subvectors $[1 \dots 1]$ or $[0 \dots 0]$ in the constraint matrix has M components and where D is the $(2N+1)$ -dimensional vector

$$\begin{bmatrix} d(-N) \\ \vdots \\ d(-1) \\ d(0) \\ d(1) \\ \vdots \\ d(N) \end{bmatrix} = \begin{bmatrix} 0 \\ \vdots \\ 0 \\ 1 \\ 0 \\ \vdots \\ 0 \end{bmatrix}$$

corresponding to a white frequency response in the look direction. Symbolically, the constraint matrix equation may be written $CA=D$, where C is the $2N+1$ by $M(2N+1)$ constraint matrix and A is the $M(2N+1)$ -dimensional adaptive filter vector. The adaptive filter must move in the direction opposite the gradient

$$\nabla \left[\epsilon^2(t) - \Lambda^T (D - CA) \right] \approx 2XX^T A - 2V + C^T \Lambda ,$$

where Λ is the Lagrangian multiplier vector

$$\Lambda = \begin{bmatrix} \lambda(-N) \\ \vdots \\ \lambda(-1) \\ \lambda(0) \\ \lambda(1) \\ \vdots \\ \lambda(N) \end{bmatrix} .$$

The update equation is

$$A(t + \Delta t) = A - \mu(t) \left[2XX^T A - 2V + C^T \Lambda \right] ,$$

and the Lagrangian multiplier vector is determined by premultiplying this equation by the constraint matrix C:

$$D = CA(t + \Delta t) = CA - \mu(t) \left[2CXX^T A - 2CV + CC^T \Lambda \right].$$

Rearrangement of this equation yields

$$\mu(t) CC^T \Lambda = [CA - D] + 2\mu(t) [CV - CXX^T A],$$

or

$$\Lambda = 2 \left(CC^T \right)^{-1} [CV - CXX^T A],$$

so that the adaptive filter update equation is

$$A(t + \Delta t) - A(t) = 2\mu(t) \left[C^T \left(CC^T \right)^{-1} C - I \right] [XX^T A - V].$$

The matrix CC^T is the $(2N+1)$ by $(2N+1)$ diagonal matrix

$$\begin{bmatrix} M & 0 & \dots & 0 \\ 0 & M & 0 & \dots & 0 \\ \vdots & \vdots & \vdots & \vdots & \vdots \\ 0 & \dots & 0 & M & 0 \\ 0 & \dots & 0 & 0 & M \end{bmatrix}$$

and the matrix $C^T \left(CC^T \right)^{-1} C$ is the $M(2N+1)$ by $M(2N+1)$ matrix

$$\begin{bmatrix}
 \left[\frac{1}{M} J_M \right] & \left[\begin{smallmatrix} 0 & \dots & 0 \\ \vdots & \ddots & \vdots \\ 0 & \dots & 0 \end{smallmatrix} \right] & \dots & \dots & \dots & \left[\begin{smallmatrix} 0 & \dots & 0 \\ \vdots & \ddots & \vdots \\ 0 & \dots & 0 \end{smallmatrix} \right] \\
 \left[\begin{smallmatrix} 0 & \dots & 0 \\ \vdots & \ddots & \vdots \\ 0 & \dots & 0 \end{smallmatrix} \right] & \left[\frac{1}{M} J_M \right] & \left[\begin{smallmatrix} 0 & \dots & 0 \\ \vdots & \ddots & \vdots \\ 0 & \dots & 0 \end{smallmatrix} \right] & \dots & \dots & \left[\begin{smallmatrix} 0 & \dots & 0 \\ \vdots & \ddots & \vdots \\ 0 & \dots & 0 \end{smallmatrix} \right] \\
 \left[\begin{smallmatrix} 0 & \dots & 0 \\ \vdots & \ddots & \vdots \\ 0 & \dots & 0 \end{smallmatrix} \right] & \dots & \dots & \left[\frac{1}{M} J_M \right] & \left[\begin{smallmatrix} 0 & \dots & 0 \\ \vdots & \ddots & \vdots \\ 0 & \dots & 0 \end{smallmatrix} \right] & \left[\begin{smallmatrix} 0 & \dots & 0 \\ \vdots & \ddots & \vdots \\ 0 & \dots & 0 \end{smallmatrix} \right] \\
 \left[\begin{smallmatrix} 0 & \dots & 0 \\ \vdots & \ddots & \vdots \\ 0 & \dots & 0 \end{smallmatrix} \right] & \dots & \dots & \left[\begin{smallmatrix} 0 & \dots & 0 \\ \vdots & \ddots & \vdots \\ 0 & \dots & 0 \end{smallmatrix} \right] & \left[\frac{1}{M} J_M \right] & \left[\begin{smallmatrix} 0 & \dots & 0 \\ \vdots & \ddots & \vdots \\ 0 & \dots & 0 \end{smallmatrix} \right]
 \end{bmatrix}$$

where each of the $2N+1$ submatrices J_M is an M by M matrix with each element equal to one. Premultiplication of any M $(2N+1)$ -dimensional column vector by the matrix C produces a column vector where all M elements in each of the $2N+1$ subvectors are identical and equal to the average of the corresponding elements in the original column vector. As a result, the adaptive filter update equation reduces to

$$A(t + \Delta t) - A(t) = 2\mu(t) \left[y(t) (\bar{X} - X) - (\bar{V} - V) \right],$$

where each element of the vector

$$\bar{V} = \begin{bmatrix} \bar{v}(t+N) \\ \vdots \\ \bar{v}(t+N) \\ \vdots \\ \bar{v}(t) \\ \vdots \\ \bar{v}(t) \\ \vdots \\ \bar{v}(t-N) \\ \vdots \\ \bar{v}(t-N) \end{bmatrix}$$

is equal to

$$\bar{v}(t-j) = \frac{1}{M} \sum_{i=1}^M \overline{x_i(t-j) s(t)}$$

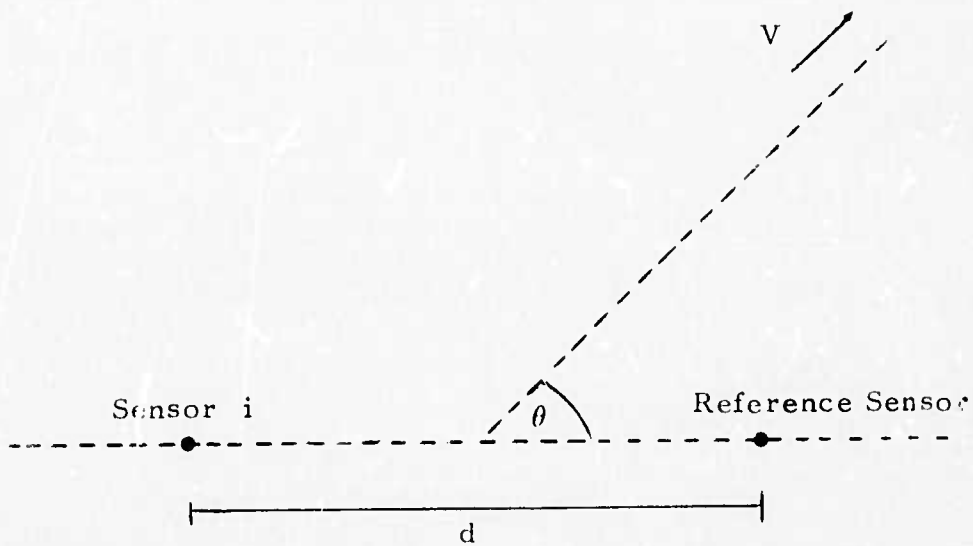
If the adaptive filter vector A initially satisfies the constraint matrix equation $CA = D$, the adaptive update equation produces adaptive filter vectors A which also satisfy the constraint equation. Because of computer roundoff error, however, the filter vector A must periodically be adjusted to satisfy the constraints.

C. ESTIMATION OF THE CROSSCORRELATION VECTOR

Since seismic adaptive processing must be performed in the time domain to obtain continuous time traces, the technique described in this subsection computes the signal model crosscorrelation function components $\overline{x_i(t-j) s(t)}$ of the vector $V = \overline{Xs(t)}$ directly in the time domain as a function of the time lag τ between the signal as seen by the reference sensor and the signal as seen by the i -th sensor.

If the power spectrum of the signal were white, the required cross-correlation function would simply be the probability density function $p(\tau)$ for the signal's time lag τ between the reference sensor and the i -th sensor. For a given distance d between the two sensors, the probability density function for $\tau = d \cos \theta / V$ depends on the joint probability distribution for θ and V , where θ is the arrival angle of the signal and V is the apparent velocity of propagation (see Figure II-1).

In order to reflect the signal power spectrum, the crosscorrelation function components $\overline{x_i(t-j) s(t)}$ are obtained by convolving the probability density function $p(\tau)$ for the specified distributed signal model with the autocorrelation function corresponding to the estimated signal power spectrum.



- θ is, for incoming energy, the arrival angle (in the plane of the array) relative to the line joining the two sensors
- V is the apparent velocity of propagation with respect to the plane of the array
- d is the distance between the two sensors
- τ is the time lag of incoming energy between the two sensors

$$\tau = \frac{d \cos \theta}{V}$$

FIGURE II-1
 DIAGRAMMATIC REPRESENTATION OF THE FACTORS DETERMINING
 THE TIME LAG OF THE SIGNAL BETWEEN TWO SENSORS

By choosing the power spectrum of the data as the model for the signal spectrum, the adaptive beamformer can be made to function solely as a directional-filtering processor.

For array sensors with well-equalized signal outputs, the average autocorrelation function across channels can serve as a model for the signal autocorrelation function:

$$\overline{s(t-k) s(t)} \approx \frac{1}{M} \sum_{m=1}^M \overline{x_m(t-k) x_m(t)} \approx \frac{1}{M} \sum_{m=1}^M x_m(t-k) x_m(t) \quad .$$

If the sensor responses differ by a simple scale factor, then an amplitude correction can be made:

$$\overline{s_i(t-k) s_i(t)} \approx \frac{1}{M} \sum_{m=1}^M x_m(t-k) x_m(t) \sqrt{\frac{\varphi_{ii}(0)}{\frac{1}{M} \sum_{m=1}^M \varphi_{mm}(0)}} \quad ,$$

where $\varphi_{ii}(0)$ and $\varphi_{mm}(0)$ denote the average power for the channels denoted by the subscripts i and m , respectively. (Since the crosscorrelation function $\overline{x_i(t-j) s(t)}$ is being estimated and the strength of the i -th sensor affects only the term $x_i(t-j)$, only an amplitude correction is made instead of a power correction.) For good results in eliminating the variations in sensor response, the power ratios $\varphi_{ii}(0)/\varphi_{mm}(0)$ need to be reasonably stable.

In the later sections of this report, formulas for the probability density function $p(\tau)$ will provide expressions for $p(\tau)$ as a continuous function of the time lag τ . The nonzero values of $p(\tau)$ lie within the interval

$$-\frac{d_{\max}}{V_{\min}} \leq \tau \leq \frac{d_{\max}}{V_{\min}} \quad ,$$

where d_{\max} is the maximum distance to the reference sensor and V_{\min} is the minimum apparent propagation velocity across the plane of the array, so that the frequency bandwidth for $p(\tau)$ is infinite. On the other hand, the autocorrelation function to be convolved with $p(\tau)$ in estimating $\overline{x_1(t-j) s(t)}$ is available only at integer multiples of the sampling interval Δt . In well-designed processing systems, spectra of signals and noise lie predominantly within the frequency band

$$-\frac{W}{2} \leq f \leq \frac{W}{2} ,$$

where $W = 1/\Delta t$ is the bandwidth corresponding to the sampling interval Δt , and it is not a bad approximation to assume that the spectrum of the data lies entirely within the band indicated. If the unmodified probability density function $p(\tau)$ were sampled and then convolved with the available values of the estimated signal autocorrelation function, then the frequency components of $p(\tau)$ outside the sampling bandwidth would, in effect, alias back into that bandwidth. A remedy for this problem is to compute a continuous convolution of $p(\tau)$ with

$$\text{sinc } W\tau = \begin{cases} 1 & \text{if } \tau = 0 \\ \frac{\sin \pi W\tau}{\pi W\tau} & \text{if } \tau \neq 0 \end{cases}$$

at integer multiples of the sampling interval Δt by numerical integration. The number of computed values should be sufficient to extend at least beyond all lags τ for which $p(\tau)$ is nonzero. Convolution with $\text{sinc } W\tau$ removes from $p(\tau)$ all spectral components outside the sampling bandwidth. If an infinite-length version of this bandlimited and sampled version of $p(\tau)$ were convolved with an infinite-length sampled autocorrelation function estimate, the result would

be the true sampled convolution of the probability density function $p(\tau)$ with the bandlimited autocorrelation function estimate. In practice, of course, both of these functions must be truncated to a finite length. If the point length is $2L+1$ for the modified version of $p(\tau)$ and $2(N+L)+1$ for the autocorrelation function estimate, then the Fourier transform of the $(2N+1)$ -point-long convolution output is the desired signal-model crosspower spectrum convolved with $\left[\sin \pi(2L+1) f \Delta t \right] / \left[\sin \pi f \Delta t \right]$, which is the Fourier transform of the $(2L+1)$ -point-long sampling function for the modified probability density function $p(\tau)$. If the number of points $2L+1$ is sufficiently large and the estimated signal-model power spectrum is sufficiently smooth, the signal-model crosscorrelation function estimates for $\overline{x_1(t-j) s(t)}$ will be relatively free of spectral window effects.

In the following sections, analytic derivations are given for the probability function $p(\tau)$ corresponding to specific distributed signal models. These derivations generally are obtained using a transformation from the specified velocity-azimuth probability distribution to a new two-dimensional space where the time lag τ is one of the coordinates.

SECTION III
INVERSE VELOCITY SPACE MODELS

A. BASIC APPROACH

In this section, the signal-model probability distributions are specified as a function of the two-dimensional inverse velocity vector

$$\vec{u} = \frac{\vec{V}}{\vec{V} \cdot \vec{V}},$$

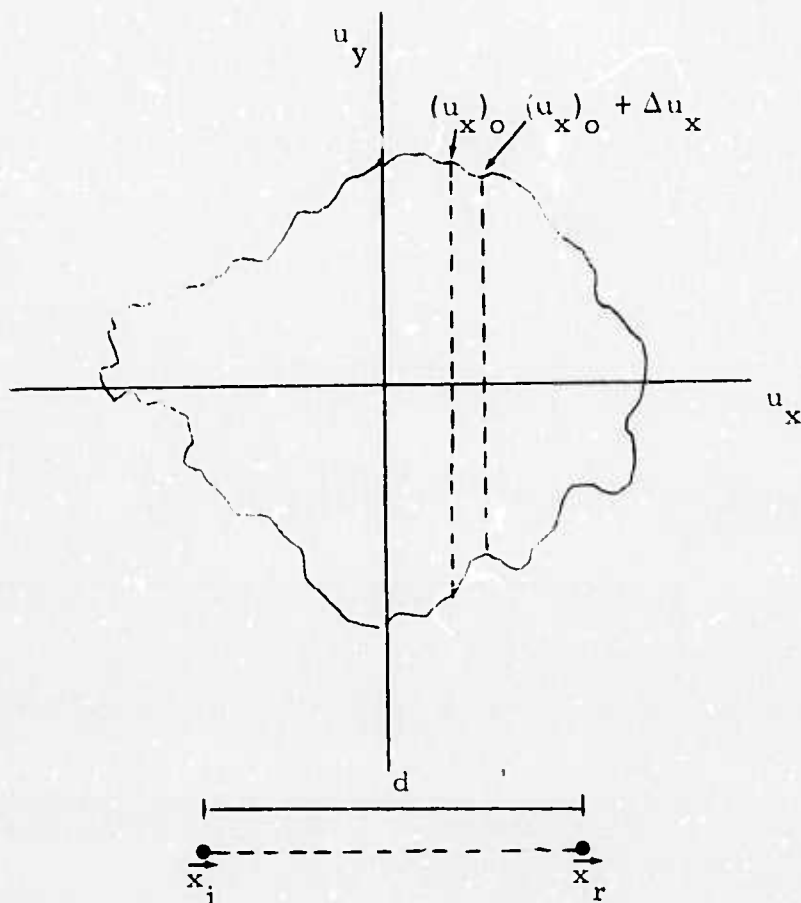
where \vec{V} is the incoming energy's apparent velocity in the plane of the array. The coordinate system axes are oriented so that the u_x coordinate points in the same direction as the line from the i -th sensor to the reference sensor (as shown in Figure III-1). The time lag τ corresponding to a particular value of \vec{u} is

$$\tau = d u_x,$$

where d is the distance between the two sensors, and

$$\frac{du_x}{d\tau} = \frac{1}{d}.$$

The probability density function $p(\tau_0)$ is determined by taking the limit as $\Delta\tau$ approaches zero for the quantity $(1/\Delta\tau)$ times the probability between τ_0 and $\tau_0 + \Delta\tau$:



- \vec{x}_i is the vector location of the i -th sensor
- \vec{x}_r is the vector location of the reference sensor
- d is the distance between the two sensors

$$\vec{u} = \frac{\vec{V}}{\vec{V} \cdot \vec{V}}$$

- \vec{u} is the inverse velocity vector corresponding to the apparent velocity across the array
- \vec{V} is the incoming energy's apparent velocity in the plane of the array

FIGURE III-1
THE BASIC INVERSE VELOCITY SPACE MODEL

$$\begin{aligned}
p(\tau_0) &= \lim_{\Delta\tau \rightarrow 0} \left\{ \frac{P(\tau_0 \leq \tau \leq \tau_0 + \Delta\tau)}{\Delta\tau} = \frac{P\left[(u_x)_0 \leq u_x \leq (u_x)_0 + \Delta u_x\right]}{\Delta\tau} \right\} \\
&= \lim_{\Delta\tau \rightarrow 0} \left[\frac{\int_{-\infty}^{\infty} p\left[(u_x)_0, u_y\right] du_y}{\Delta\tau} \Delta u_x \right] \\
&= \frac{1}{d} \int_{-\infty}^{\infty} p\left[(u_x)_0, u_y\right] du_y .
\end{aligned}$$

B. DISK MODEL

For this model, the probability density is uniform on the disk $|\vec{u}| < u_{\max}$, where $u_{\max} = 1/V_{\min}$ and V_{\min} is the minimum apparent velocity across the array:

$$p(u_x, u_y) = \begin{cases} \frac{1}{\pi u_{\max}^2} & \text{if } |\vec{u}| < u_{\max} \\ 0 & \text{if } |\vec{u}| > u_{\max}. \end{cases}$$

The probability density function $p(\tau)$ for the time lag τ is

$$\begin{aligned}
p(\tau) &= \frac{2\sqrt{u_{\max}^2 - u_x^2}}{\pi u_{\max}^2 d} \\
&= \frac{2}{\pi u_{\max}^2 d} \sqrt{1 - \left(\frac{u_x}{u_{\max}}\right)^2} \\
&= \frac{2V_{\min}}{\pi d} \sqrt{1 - \left(\frac{V_{\min}\tau}{d}\right)^2}
\end{aligned}$$

for $|\tau| \leq d/V_{\min}$ and zero elsewhere. Figure III-2 displays $p(\tau)$ for this model, whose principal application arises in connection with infinite-velocity P waves.

C. ANNULAR MODEL

In this model, the probability density is uniform on the annulus $u_{\min} < |\vec{u}| < u_{\max}$, where $u_{\max} = 1/V_{\min}$, $u_{\min} = 1/V_{\max}$, and V_{\min} and V_{\max} are the minimum and maximum apparent velocities, respectively, across the array:

$$p(u_x, u_y) = \begin{cases} \frac{1}{\pi(u_{\max}^2 - u_{\min}^2)} & \text{if } u_{\min} < |\vec{u}| < u_{\max} \\ 0 & \text{if } |\vec{u}| < u_{\min} \text{ or } |\vec{u}| > u_{\max} \end{cases}$$

The probability density function $p(\tau)$ for the time lag τ is

$$p(\tau) = \begin{cases} \frac{2}{\pi(u_{\max}^2 - u_{\min}^2)d} \left[\sqrt{u_{\max}^2 - u_x^2} - \sqrt{u_{\min}^2 - u_x^2} \right] & \text{if } u_x \leq u_{\min} \\ \frac{2}{\pi(u_{\max}^2 - u_{\min}^2)d} \sqrt{u_{\max}^2 - u_x^2} & \text{if } u_{\min} \leq u_x \leq u_{\max} \\ \frac{2}{\pi d \left(\frac{1}{V_{\min}^2} - \frac{1}{V_{\max}^2} \right)} \left[\frac{1}{V_{\min}} \sqrt{1 - \left(\frac{V_{\min} \tau}{d} \right)^2} - \frac{1}{V_{\max}} \sqrt{1 - \left(\frac{V_{\max} \tau}{d} \right)^2} \right] & \text{if } |\tau| \leq \frac{d}{V_{\max}} \\ \frac{2}{\pi d \left(\frac{1}{V_{\min}^2} - \frac{1}{V_{\max}^2} \right)} \left[\frac{1}{V_{\min}} \sqrt{1 - \left(\frac{V_{\min} \tau}{d} \right)^2} \right] & \text{if } \frac{d}{V_{\max}} \leq |\tau| \leq \frac{d}{V_{\min}} \end{cases}$$

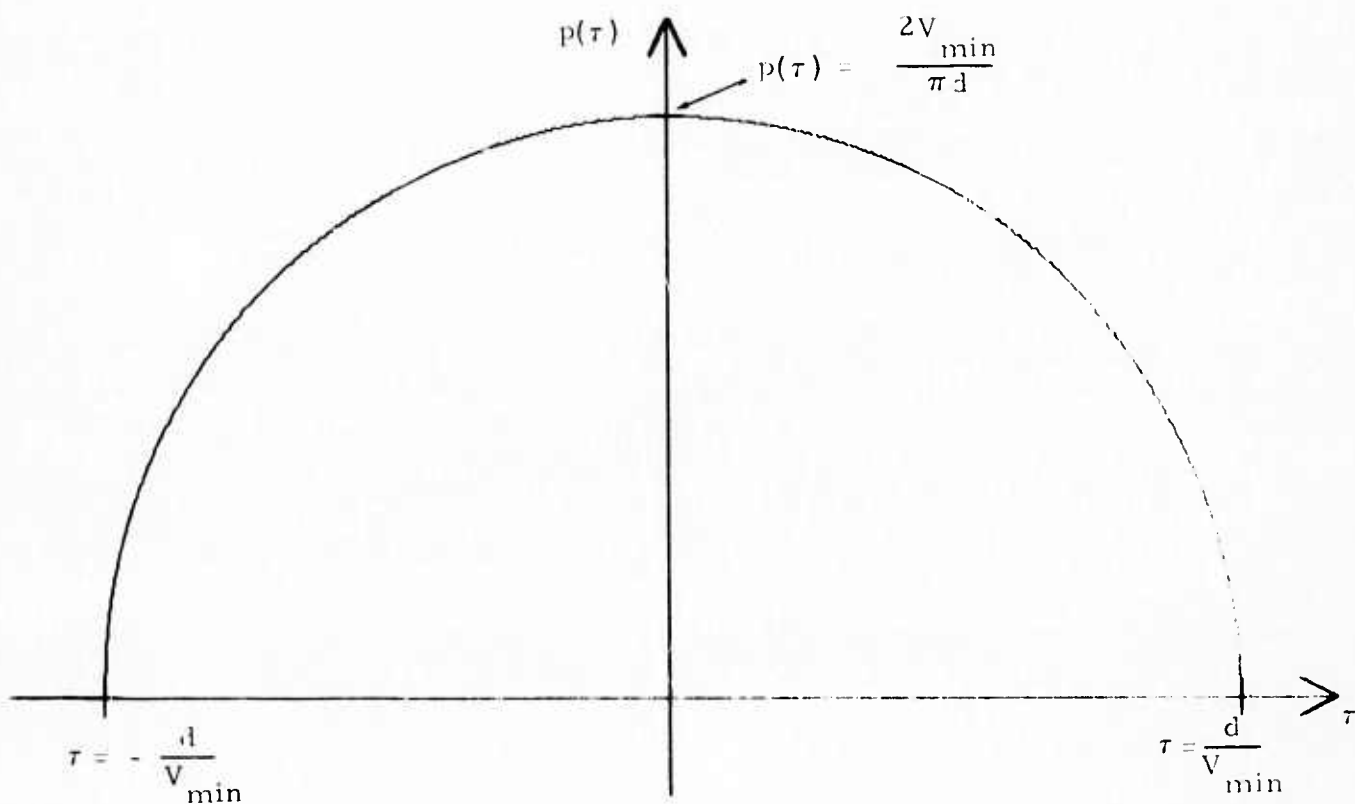


FIGURE III-2
 TIME-LAG PROBABILITY DENSITY FUNCTION
 FOR THE INVERSE VELOCITY SPACE DISK MODEL

and zero for $|\tau| > d/V_{\min}$. Figure III-3 presents $p(\tau)$ for the annular model at nine values of V_{\min}/V_{\max} .

D. SECTOR-OF-ANNULUS MODEL

In this model, the probability density is uniform on the sector of the annulus $u_{\min} < |\vec{u}| < u_{\max}$ between θ_{\min} and θ_{\max} , which are the minimum and maximum arrival angles relative to the line joining the i -th sensor and the reference sensor. That is to say,

$$p(u_x, u_y) = \begin{cases} \frac{2}{(\theta_{\max} - \theta_{\min})(u_{\max}^2 - u_{\min}^2)} & \text{if } u_{\min} < |\vec{u}| < u_{\max} \\ & \text{and } \theta_{\min} < \theta < \theta_{\max} \\ 0 & \text{otherwise.} \end{cases}$$

Breaking up the angular range $\theta_{\min} < \theta < \theta_{\max}$ into sections bounded by the transition angles $-\pi, 0, \pi$ encountered as θ sweeps from θ_{\min} to θ_{\max} considerably simplifies the determination of $p(\tau)$. If θ_{\min} and θ_{\max} are specified so that $-2\pi \leq \theta_{\min} < 2\pi$, $-2\pi < \theta_{\max} \leq 2\pi$, and $\theta_{\min} < \theta_{\max} \leq \theta_{\min} + 2\pi$, then there are no more than three sections, each lying either in the first and second quadrants or in the third and fourth quadrants. Sections can be mapped into the first and second quadrants in such a way that the probability density as a function of τ is unaffected. Figure III-4 depicts a procedure for determining the minimum angle α and the maximum angle β of each section after the appropriate mapping onto the first and second quadrants. Once the subdivision of the angular range $\theta_{\min} < \theta < \theta_{\max}$ and the mapping onto the first and second quadrants have been completed, the probability density function $p(\tau)$ is determined by adding the contributions from the appropriate sections at the time lag τ . If the minimum angle α and the maximum angle β after mapping onto the first and

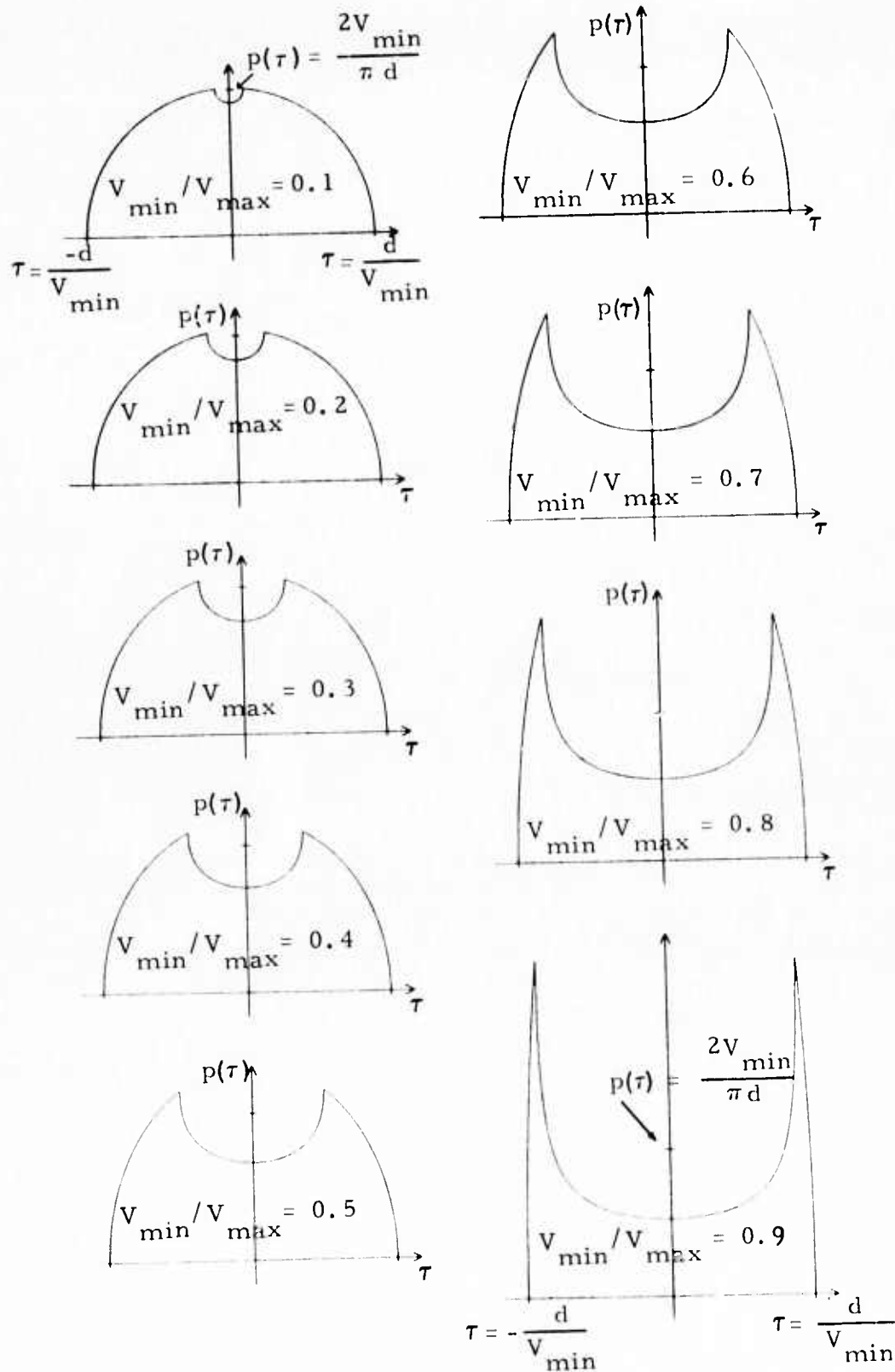


FIGURE III-3

TIME-LAG PROBABILITY DENSITY FUNCTION
FOR THE INVERSE VELOCITY SPACE ANNULAR MODEL
AT NINE VALUES OF V_{\min}/V_{\max}

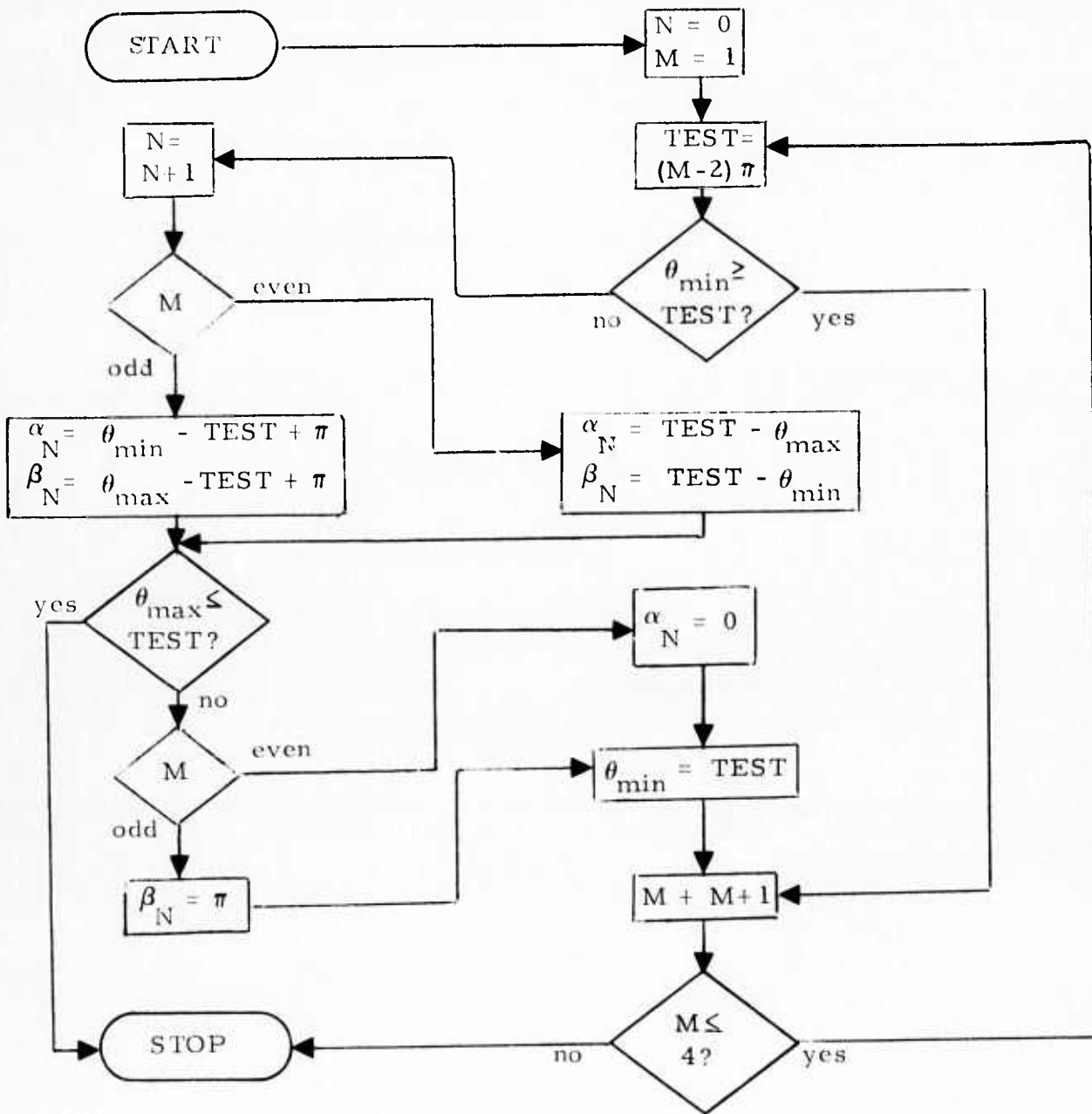


FIGURE III-4

PROCEDURE FOR MAPPING ANGLES BETWEEN
 θ_{\min} AND θ_{\max} ONTO FIRST AND SECOND QUADRANTS

second quadrants both lie in the same quadrant and the annulus between u_{\min} and u_{\max} is thick enough, there will be a range of u_x for which the extremal values of u_y are located on the section boundaries $\vec{u} = (u \cos \beta, u \sin \beta)$ and $\vec{u} = (u \cos \alpha, u \sin \alpha)$. On the other hand, if α lies in the first quadrant and β in the second quadrant or if the annulus is thin enough, there will be a range of u_x for which the extremal values of u_y lie on the circles $|\vec{u}| = u_{\max}$ and $|\vec{u}| = u_{\min}$. Figure III-5 illustrates these two possibilities when α and β both lie in the first quadrant. The case shown in Figure III-5(a) corresponds to the condition $u_{\max} \cos \beta < u_{\min} \cos \alpha$, while the case shown in Figure III-5(b) corresponds to the condition $u_{\min} \cos \alpha < u_{\max} \cos \beta$.

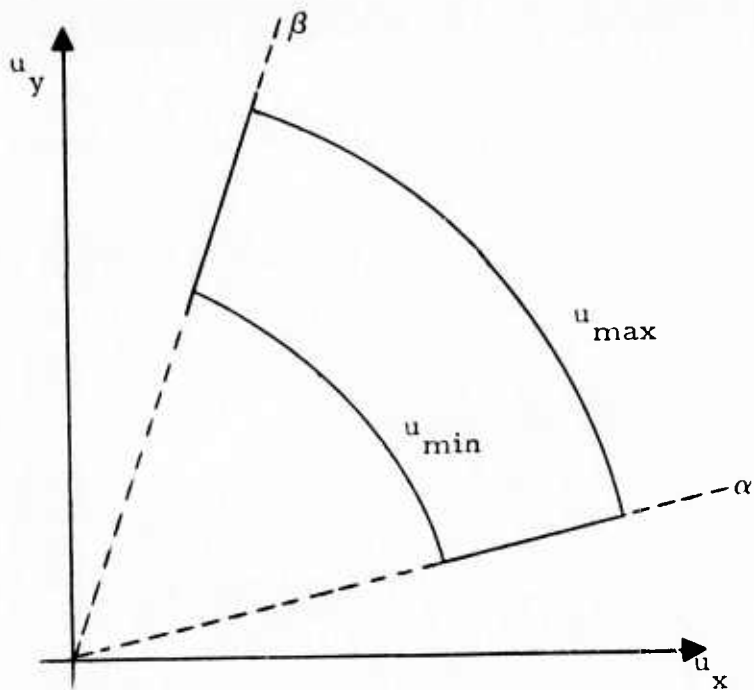
On the line $\vec{u} = (u \cos \gamma, u \sin \gamma)$, $u_x = \tau/d$ and $u_y = \tau \tan \gamma/d$, so that $u_y = \tau \tan \alpha/d$ or $u_y = \tau \tan \beta/d$ whenever a section boundary corresponds to the extremal value for u_y at the time lag τ . For any given pair of angles α and β , there are three possible u_x intervals where the formula for $p(\tau)$ is different. In the first and last of these intervals, one extremal value of u_y is on a section boundary, while the other is on a circular arc. In the middle interval, both extremal values lie either on circular arcs or on section boundaries.

Let

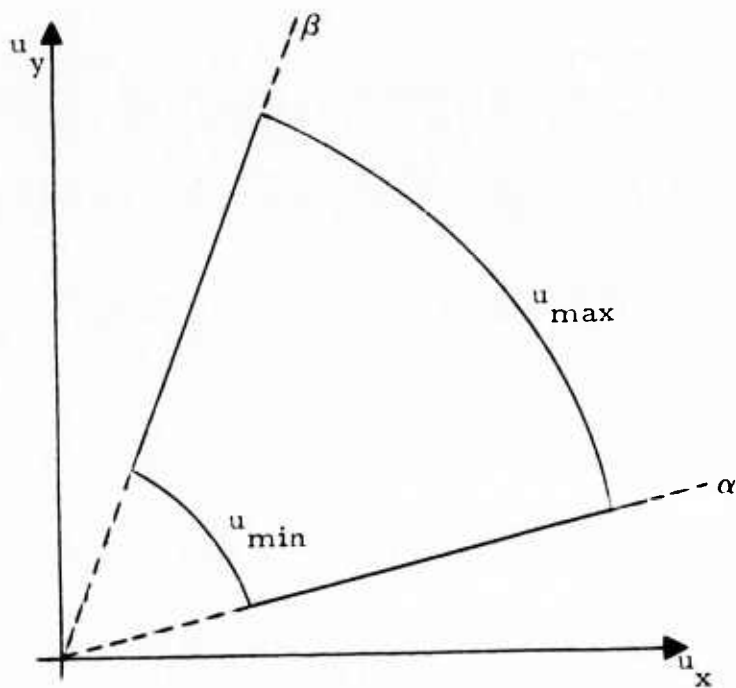
$$K = \frac{2}{d(\theta_{\max} - \theta_{\min})(u_{\max}^2 - u_{\min}^2)}$$

$$= \frac{2}{d(\theta_{\max} - \theta_{\min}) \left(\frac{1}{v_{\min}^2} - \frac{1}{v_{\max}^2} \right)}$$

If $\pi/2 < \beta$, then the first interval is $u_{\max} \cos \beta \leq u_x \leq \min(u_{\min} \cos \beta, u_{\max} \cos \alpha)$ and



(a) No Time-Lag Overlap Between Section Boundaries



(b) Time-Lag Overlap Between Section Boundaries

FIGURE III-5

THE TWO FIRST-QUADRANT POSSIBILITIES AFFECTING THE FORMULAS
FOR THE TIME-LAG PROBABILITY DENSITY FUNCTION

$$p(\tau) = K \left[\sqrt{u_{\max}^2 - u_x^2} - \frac{\tau \tan \beta}{d} \right]$$

$$= K \left[\frac{1}{V_{\min}} \sqrt{1 - \left(\frac{V_{\min} \tau}{d} \right)^2} - \frac{\tau \tan \beta}{d} \right]$$

for $(d \cos \beta / V_{\min}) \leq \tau \leq \min [(d \cos \beta / V_{\max}), (d \cos \alpha / V_{\min})]$. If $\beta < \pi / 2$, then the first interval is $u_{\min} \cos \beta \leq u_x \leq \min (u_{\max} \cos \beta, u_{\min} \cos \alpha)$ and

$$p(\tau) = K \left[\frac{\tau \tan \beta}{d} - \sqrt{u_{\min}^2 - u_x^2} \right]$$

$$= K \left[\frac{\tau \tan \beta}{d} - \frac{1}{V_{\max}} \sqrt{1 - \left(\frac{V_{\max} \tau}{d} \right)^2} \right]$$

for $(d \cos \beta / V_{\max}) \leq \tau \leq \min [(d \cos \beta / V_{\min}), (d \cos \alpha / V_{\max})]$. If $\beta = \pi / 2$, the first interval is of zero length, and the formula for the second interval should be used at $\tau = 0$. If $\max (u_{\max} \cos \beta, u_{\min} \cos \beta) \leq u_x \leq \min (u_{\max} \cos \alpha, u_{\min} \cos \alpha)$, then the extremal values of u_y in the second interval are on circular arcs and

$$p(\tau) = K \left[\sqrt{u_{\max}^2 - u_x^2} - \sqrt{u_{\min}^2 - u_x^2} \right]$$

$$= K \left[\frac{1}{V_{\min}} \sqrt{1 - \left(\frac{V_{\min} \tau}{d} \right)^2} - \frac{1}{V_{\max}} \sqrt{1 - \left(\frac{V_{\max} \tau}{d} \right)^2} \right]$$

for $\max [(d \cos \beta / V_{\min}), (d \cos \beta / V_{\max})] \leq \tau \leq \min [(d \cos \alpha / V_{\min}), (d \cos \alpha / V_{\max})]$. If $\min (u_{\max} \cos \alpha, u_{\min} \cos \alpha) \leq u_x \leq \max (u_{\max} \cos \beta, u_{\min} \cos \beta)$, then the extremal values of u_y in the second interval are on section boundaries and

$$p(\tau) = \frac{K |\tau|}{d} |\tan \beta - \tan \alpha|$$

for $\min [(d \cos \alpha / V_{\min}), (d \cos \alpha / V_{\max})] \leq \tau \leq \max [(d \cos \beta / V_{\min}), (d \cos \beta / V_{\max})]$. If the limits for the second interval are equal, then only the formulas for the first and third intervals should be used. If $\pi/2 < \alpha$, then the third interval is $\max (u_{\min} \cos \beta, u_{\max} \cos \alpha) \leq u_x \leq u_{\min} \cos \alpha$ and

$$p(\tau) = K \left[\frac{\tau \tan \alpha}{d} - \sqrt{u_{\min}^2 - u_x^2} \right]$$

$$= K \left[\frac{\tau \tan \alpha}{d} - \frac{1}{V_{\max}} \sqrt{1 - \left(\frac{V_{\max} \tau}{d} \right)^2} \right]$$

for $\max [(d \cos \beta / V_{\max}), (d \cos \alpha / V_{\min})] \leq \tau \leq (d \cos \alpha / V_{\max})$. If $\alpha < \pi/2$, then the third interval is $\max (u_{\max} \cos \beta, u_{\min} \cos \alpha) \leq u_x \leq u_{\max} \cos \alpha$ and

$$p(\tau) = K \left[\sqrt{u_{\max}^2 - u_x^2} - \frac{\tau \tan \alpha}{d} \right]$$

$$= K \left[\frac{1}{V_{\min}} \sqrt{1 - \left(\frac{V_{\min} \tau}{d} \right)^2} - \frac{\tau \tan \alpha}{d} \right]$$

for $\max [(d \cos \alpha / V_{\min}), (d \cos \alpha / V_{\max})] \leq \tau \leq (d \cos \alpha / V_{\min})$. If $\alpha = \pi/2$, then the third interval is of zero length, and the formula for the second interval should be used at $\tau = 0$.

Figures III-6 and III-7 portray the time-lag probability density function $p(\tau)$ at $V_{\min} / V_{\max} = 0.1$ and $V_{\min} / V_{\max} = 0.9$, respectively, for various 30° sectors.

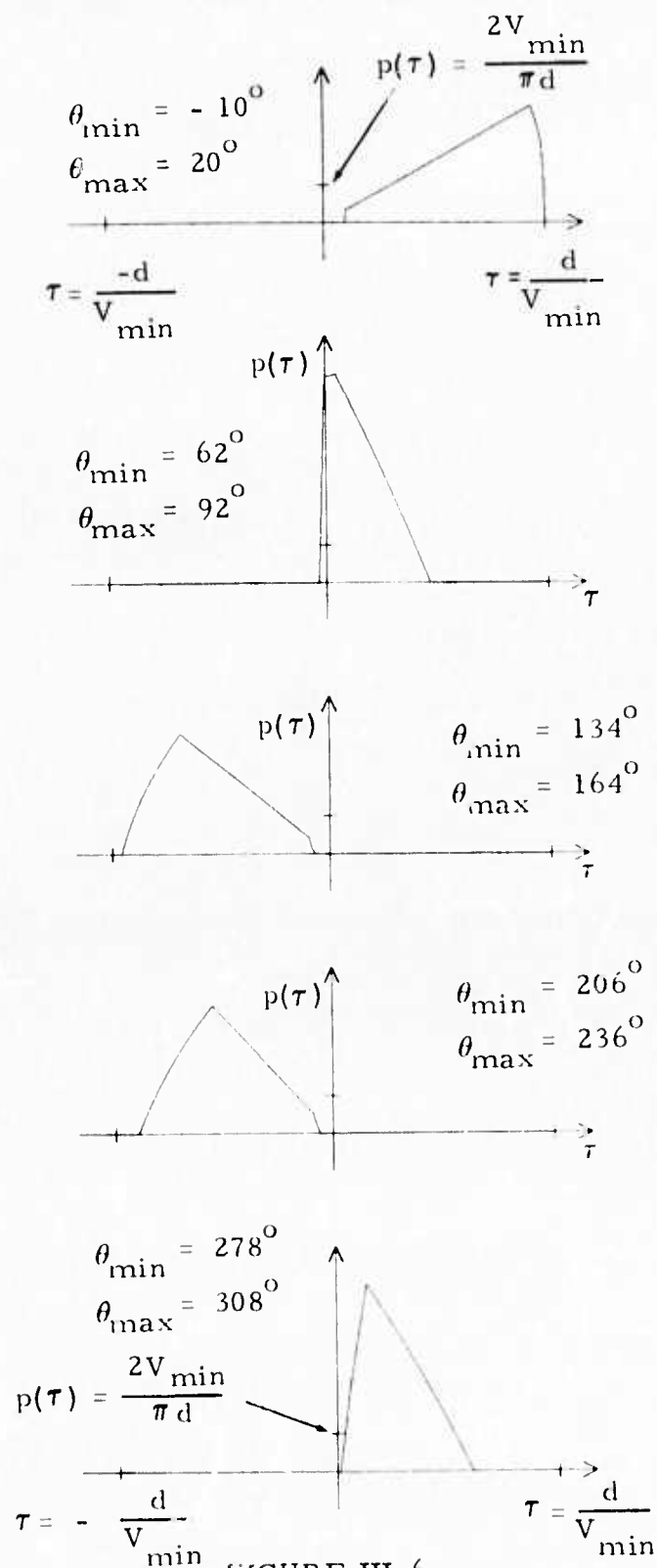


FIGURE III-6

TIME-LAG PROBABILITY DENSITY FUNCTION FOR THE INVERSE VELOCITY SPACE SECTOR-OF-ANNULUS MODEL AT $V_{\min}/V_{\max} = 0.1$ FOR VARIOUS 30° SECTORS

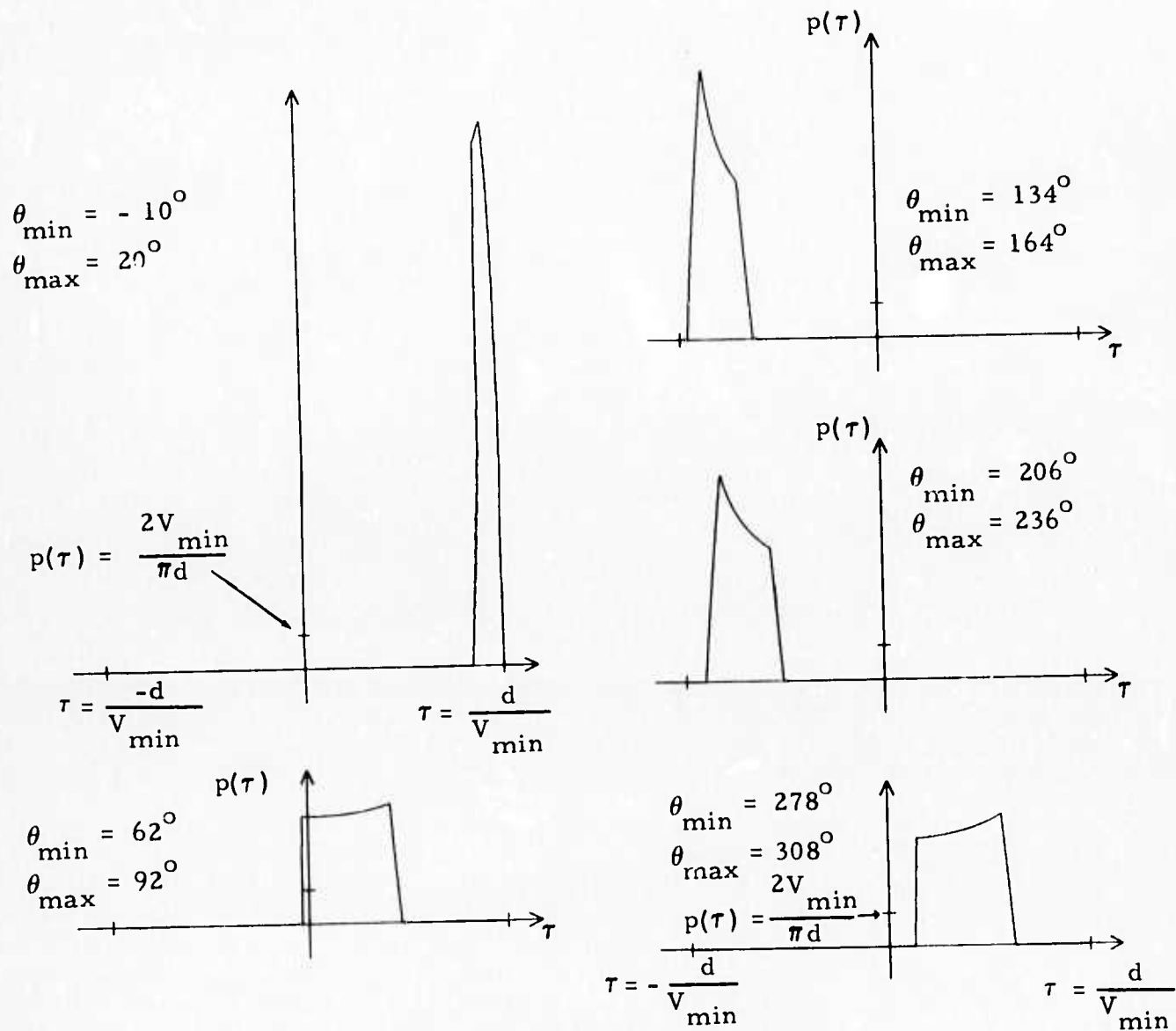


FIGURE III-7

TIME-LAG PROBABILITY DENSITY FUNCTION
 FOR THE INVERSE VELOCITY SPACE SECTOR-OF-ANNULUS MODEL
 AT $V_{\min}/V_{\max} = 0.9$ FOR VARIOUS 30° SECTORS

SECTION IV

DISTRIBUTED RING MODEL

In this form of distributed signal model, all incoming energy is concentrated at a single apparent velocity V with respect to the plane of the array. The incoming energy, however, is distributed over a range of arrival angles with respect to the line joining the i -th sensor to the reference sensor. If the probability density function $p_{\theta}(\theta)$ is known between the arrival angles $-\pi$ and π , the probability density function $p(\tau)$ for the time lag τ can be easily determined. First, a transformation from velocity-azimuth space to delay-azimuth space is made with the formula

$$\tau = \frac{d \cos \theta}{V},$$

where d is the distance between the two sensors. The line $V = \text{constant}$ is transformed into a cosine curve (as shown in Figure IV-1). For a given time lag τ , the corresponding angles are $\theta = \cos^{-1}(V\tau/d)$ and $\theta = -\cos^{-1}(V\tau/d)$.

When any time lag τ_0 is less than $-d/V$, the probability $P(\tau \leq \tau_0)$ that τ is not greater than τ_0 is the constant value zero. Correspondingly, when any time lag τ_0 is greater than d/V , the probability $P(\tau \leq \tau_0)$ is one. Thus the probability density function $p(\tau)$ is zero for $|\tau| > d/V$. Between $\tau = -d/V$ and $\tau = d/V$,

$$P(\tau \leq \tau_0) = 1 - \left\{ F_{\theta} \left[\cos^{-1} \left(\frac{V\tau_0}{d} \right) \right] - F_{\theta} \left[-\cos^{-1} \left(\frac{V\tau_0}{d} \right) \right] \right\},$$

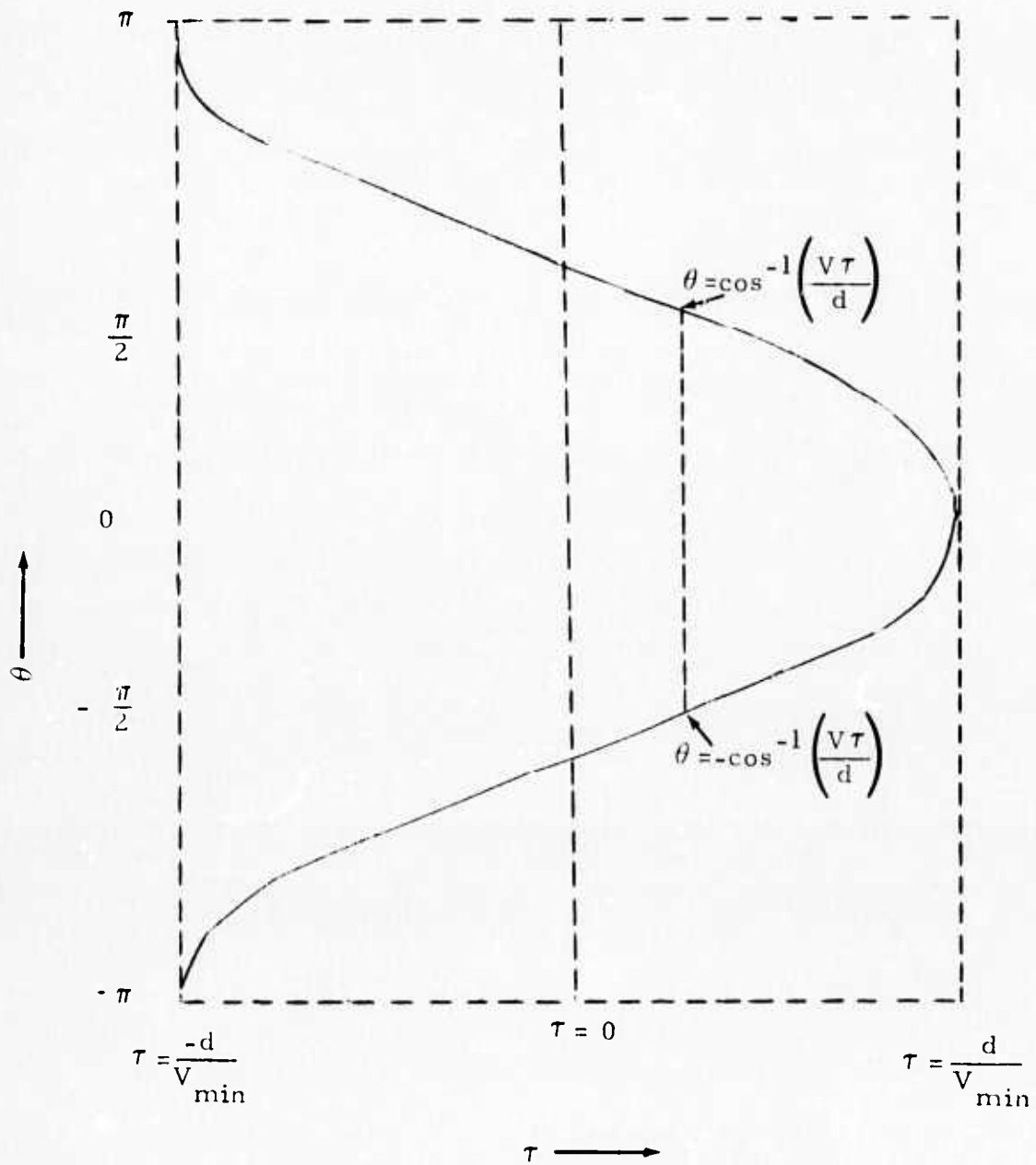


FIGURE IV-1
 TRANSFORMATION FROM VELOCITY-AZIMUTH SPACE
 TO DELAY-AZIMUTH SPACE FOR DISTRIBUTED RING MODEL

where $F_{\theta}(\theta)$ is the cumulative distribution function for the arrival angle θ . Thus, for $|\tau| < d/V$, the time-lag probability density function is

$$\begin{aligned}
 p(\tau_0) &= \frac{dP(\tau \leq \tau_0)}{d\tau_0} \\
 &= \frac{d}{d\tau_0} \left\{ 1 - F_{\theta} \left[\cos^{-1} \left(\frac{V\tau_0}{d} \right) \right] + F_{\theta} \left[-\cos^{-1} \left(\frac{V\tau_0}{d} \right) \right] \right\} \\
 &= -p_{\theta} \left[\cos^{-1} \left(\frac{V\tau_0}{d} \right) \right] \left[-\frac{1}{\sqrt{1 - (V\tau_0/d)^2}} \right] \left(\frac{V}{d} \right) \\
 &\quad + p_{\theta} \left[-\cos^{-1} \left(\frac{V\tau_0}{d} \right) \right] \left[\frac{1}{\sqrt{1 - (V\tau_0/d)^2}} \right] \left(\frac{V}{d} \right),
 \end{aligned}$$

so that

$$p(\tau) = \begin{cases} \frac{p_{\theta} \left[-\cos^{-1} \left(\frac{V\tau}{d} \right) \right] + p_{\theta} \left[\cos^{-1} \left(\frac{V\tau}{d} \right) \right]}{\sqrt{\left(\frac{d}{V} \right)^2 - \tau^2}} & \text{for } |\tau| < \frac{d}{V} \\ 0 & \text{for } |\tau| > \frac{d}{V} \end{cases} .$$

If the arrival angle probability density function $p_{\theta}(\theta)$ is nonzero when θ is an integer multiple of π , there will be a discontinuity in $p(\tau)$ at $|\tau| = d/V$: as $|\tau|$ approaches d/V from smaller absolute values, $p(\tau)$ goes to infinity; for all values of $|\tau|$ greater than d/V , on the other hand, $p(\tau)$ is zero.

Figure IV-2 depicts, for selected 30° sectors, the probability density function $p(\tau)$ corresponding to the uniform angular probability density function

$$p_\theta(\theta) = \begin{cases} \frac{1}{\theta_{\max} - \theta_{\min}} & \text{if } \theta_{\min} < \theta < \theta_{\max} \\ 0 & \text{otherwise.} \end{cases}$$

In the case where $\theta_{\min} = -10^\circ$ and $\theta_{\max} = 20^\circ$, the probability density approaches ∞ as τ approaches d/V from the left.

Figure IV-3 pictures $p(\tau)$ when the incoming energy is equally likely at all possible arrival azimuths. The time-lag probability function approaches ∞ as τ approaches $\pm d/V$ moving outward from $\tau = 0$. This figure illustrates the limiting case for the inverse velocity space model when V_{\min}/V_{\max} approaches one (compare with Figures III-2 and III-3).

Figure IV-4 represents the probability density function $p(\tau)$ for the time lag τ when the arrival-angle probability density is normally distributed about some angle θ_0 :

$$p_\theta(\theta) = \frac{1}{\sigma\sqrt{2\pi}} e^{-\frac{(\theta-\theta_0)^2}{2\sigma^2}}.$$

For this figure, the standard deviation σ is 15° . Strictly speaking, there is an infinite discontinuity at $\tau = \pm d/V$ in all cases, but the probability associated with these discontinuities is sometimes minuscule and the discontinuity for such cases is not shown in the figure.

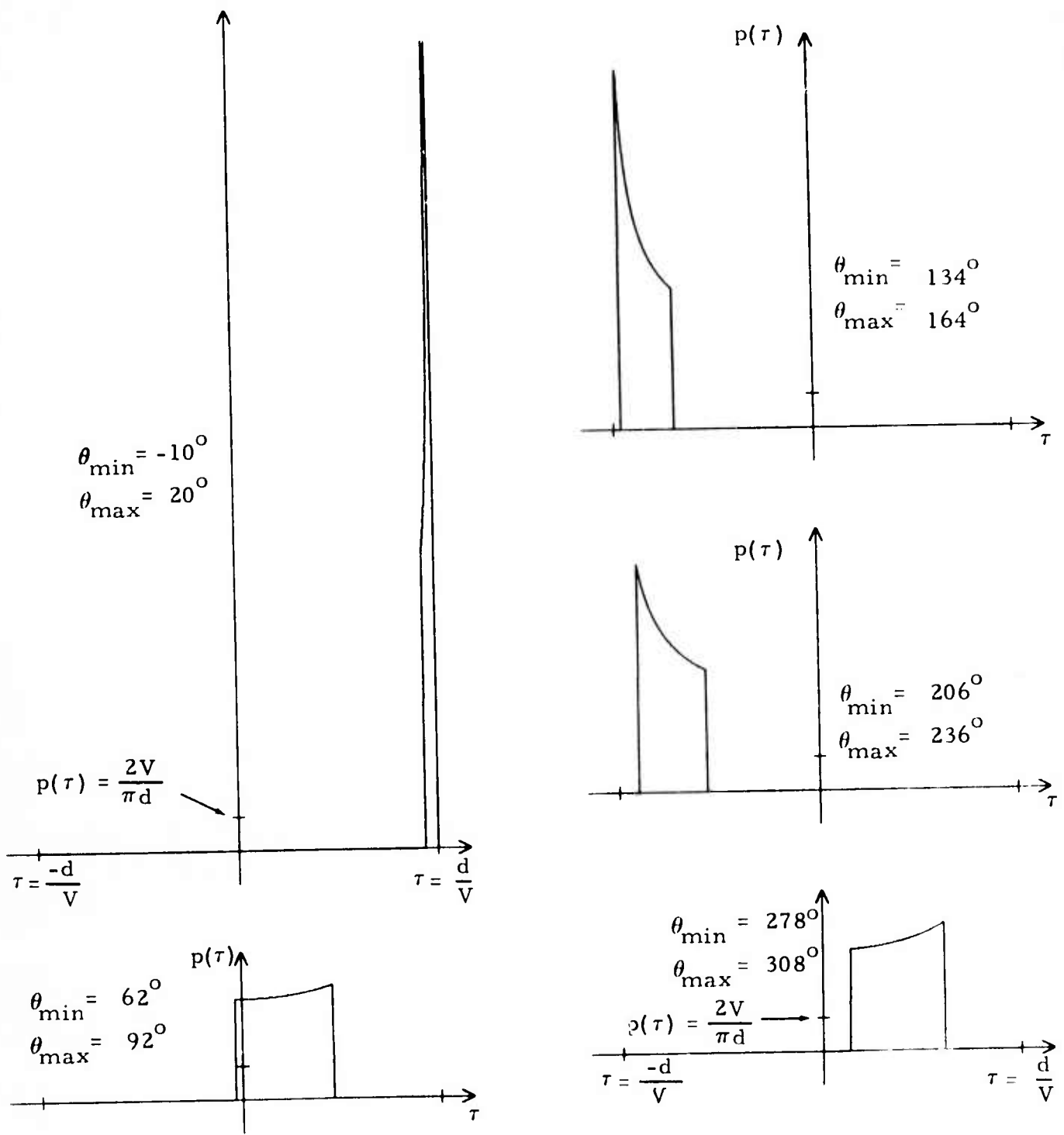


FIGURE IV-2
 TIME-LAG PROBABILITY DENSITY FUNCTION FOR THE DISTRIBUTED RING
 MODEL WITH A UNIFORM DISTRIBUTION OVER VARIOUS 30° SECTORS

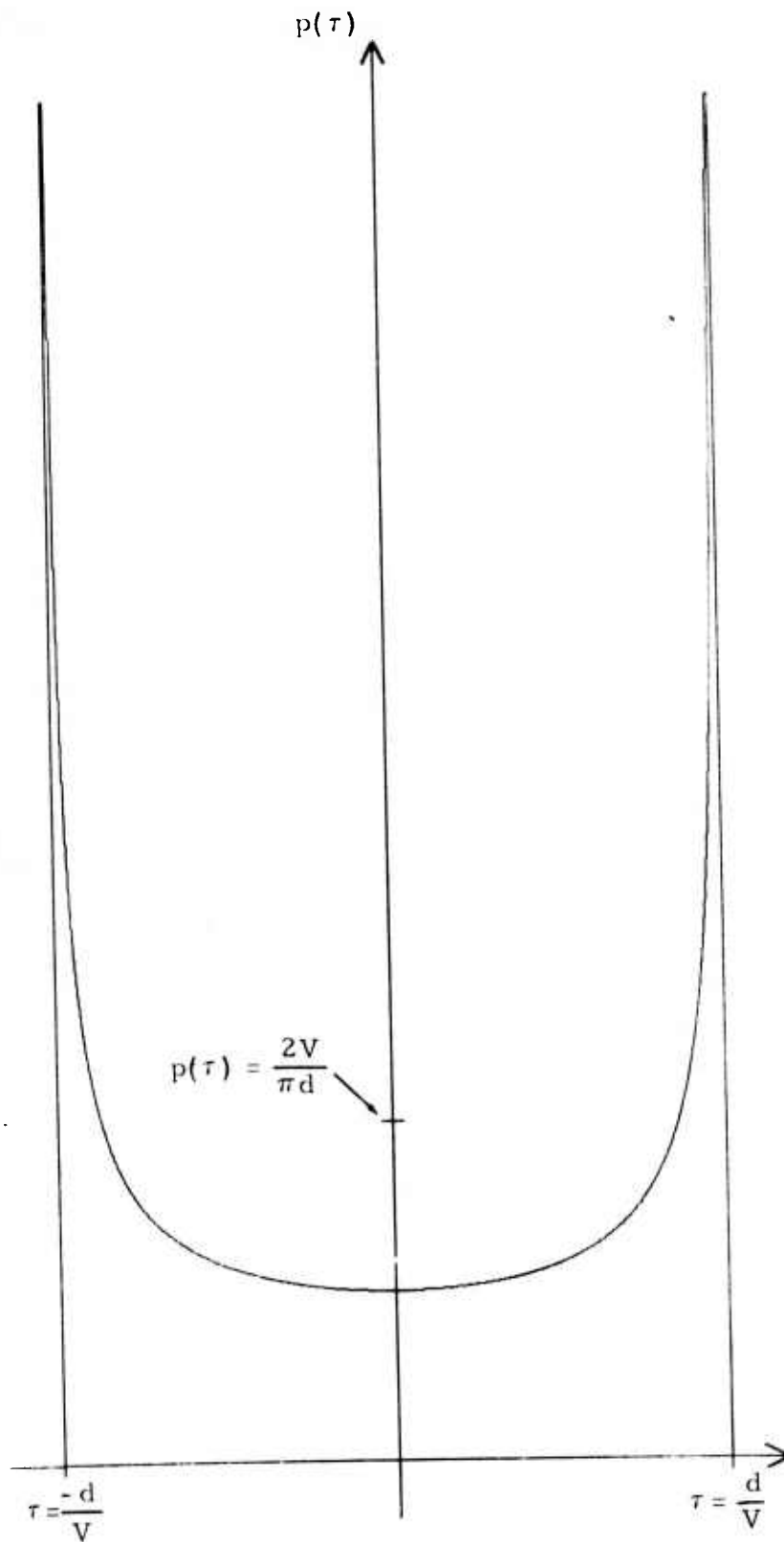


FIGURE IV-3

TIME-LAG PROBABILITY DENSITY FUNCTION FOR THE DISTRIBUTED RING MODEL WITH INCOMING ENERGY EQUALLY LIKELY AT ALL AZIMUTHS

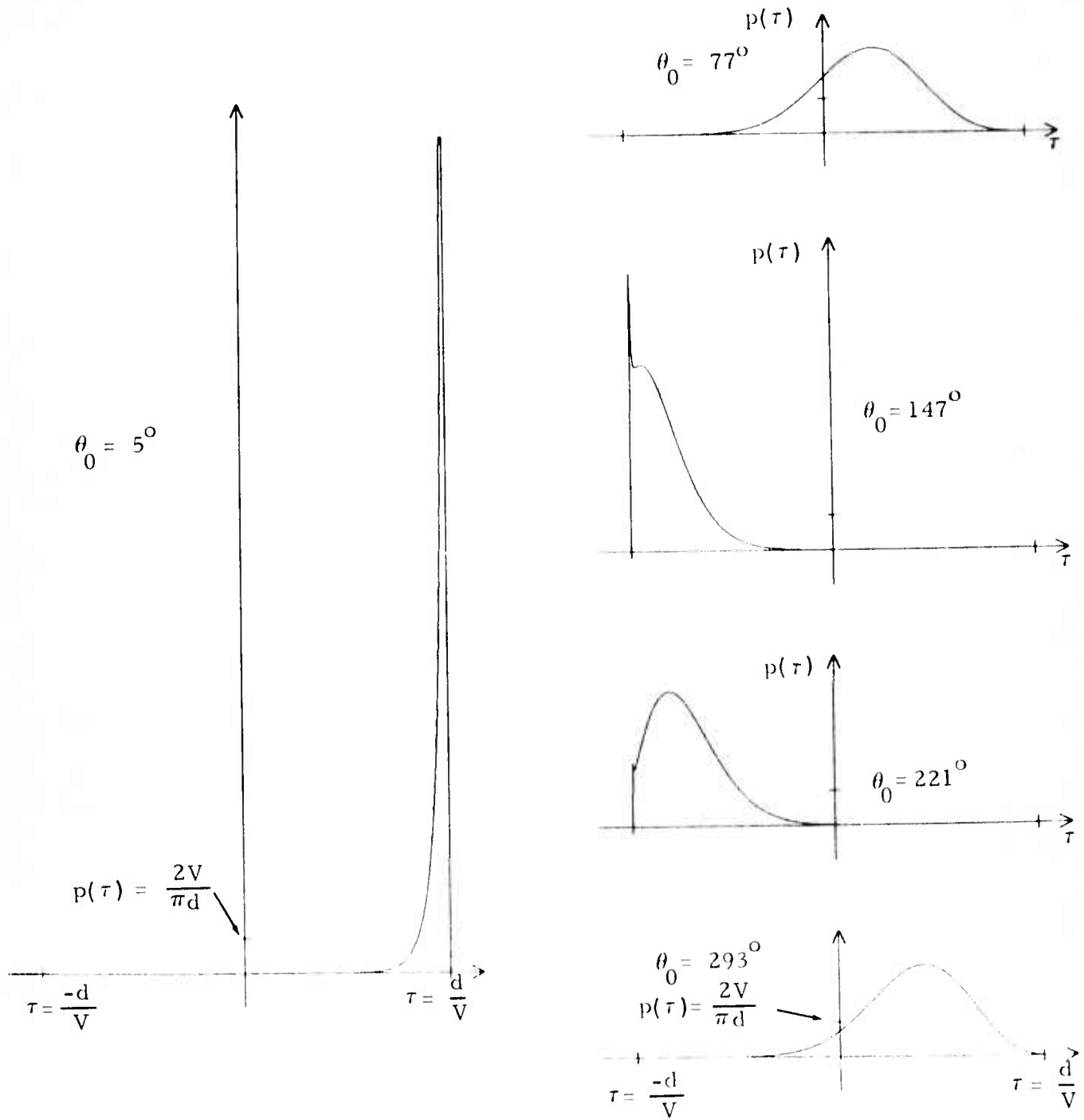


FIGURE IV-4
 TIME-LAG PROBABILITY DENSITY FUNCTION FOR THE DISTRIBUTED RING
 MODEL WITH A NORMAL DISTRIBUTION ($\sigma = 15^\circ$) PEAKING AT
 VARIOUS ANGLES

SECTION V
VELOCITY-AZIMUTH SPACE MODELS

A. BASIC APPROACH

In this section, the signal-model probability distributions are specified as a function of the apparent velocity V in the plane of the array and the arrival angle θ with respect to the line joining the i -th sensor to the reference sensor. The cumulative distribution function $F(\tau_0)$ for the time lag τ_0 , i. e., the probability $P(\tau \leq \tau_0)$ that τ is less than or equal to some arbitrary time lag τ_0 , is obtained by integrating over all points (V, θ) corresponding to time lags less than or equal to τ_0 :

$$F(\tau_0) = P(\tau \leq \tau_0) = \iint_{\tau \leq \tau_0} p(V, \theta) d\theta dV,$$

where $p(V, \theta)$ is the probability density at the point (V, θ) . The transformation of variables

$$\tau = \frac{d \cos \theta}{V} \quad \theta = \theta$$

facilitates the evaluation of the double integral above. If the probability density is nonzero only inside the rectangle specified by $V_{\min} \leq V \leq V_{\max}$ and $-\pi \leq \theta \leq \pi$, Figure V-1 illustrates the corresponding area in (τ, θ) space. The shaded area corresponds to the specified rectangle in (V, θ) space. After transformation, the cumulative distribution function $F(\tau_0)$ is

$$F(\tau_0) = \int_{-\infty}^{\tau_0} \int_{-\pi}^{\pi} p(V, \theta) |J(\tau, \theta)| d\theta d\tau,$$

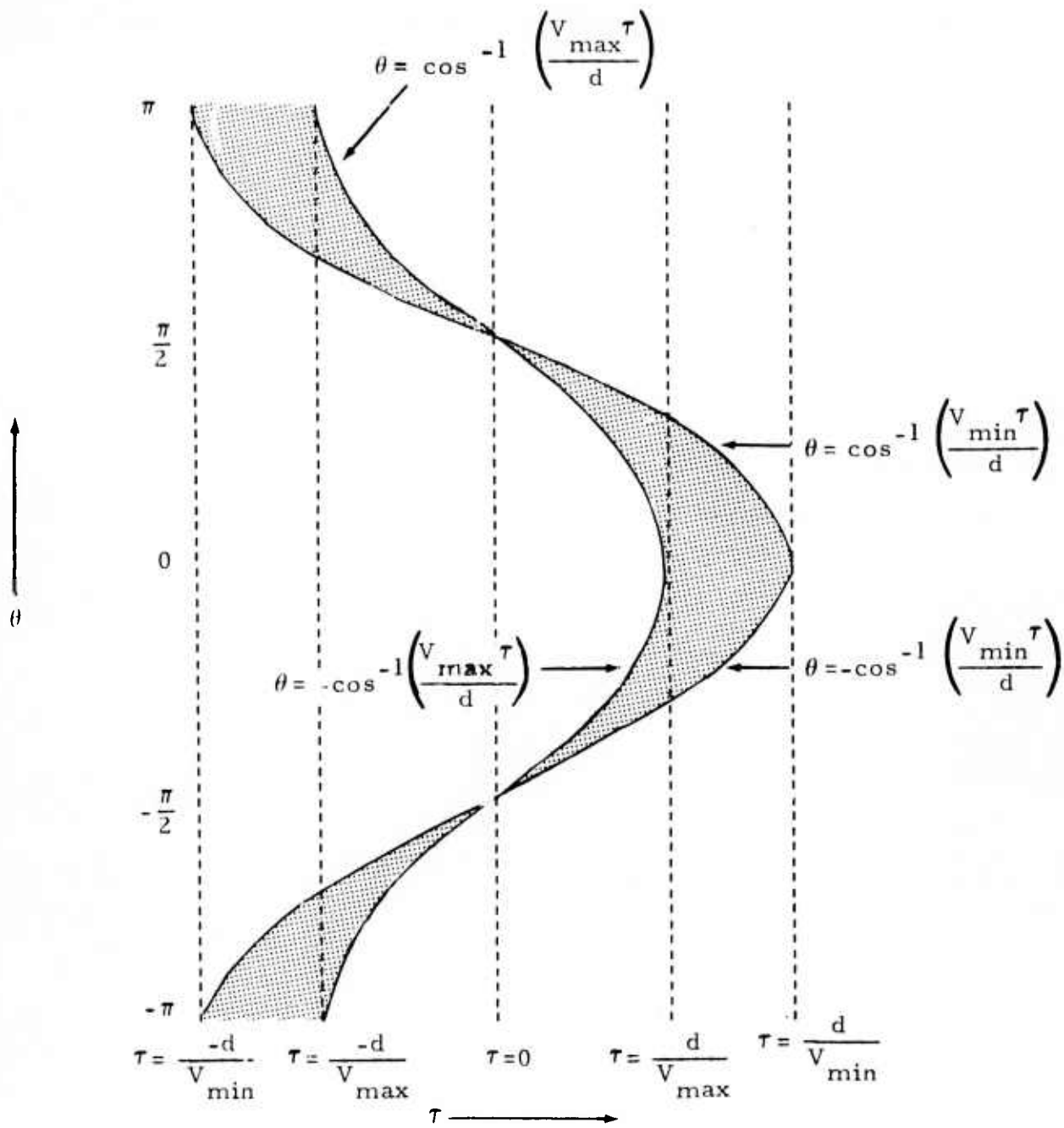


FIGURE V-1
 TRANSFORMATION FROM (V, θ) SPACE TO (τ, θ) SPACE

where $J(\tau, \theta)$ is the Jacobian

$$\begin{aligned}
 J(\tau, \theta) &= \begin{vmatrix} \frac{\partial V}{\partial \tau} & \frac{\partial V}{\partial \theta} \\ \frac{\partial \theta}{\partial \tau} & \frac{\partial \theta}{\partial \theta} \end{vmatrix} \\
 &= \begin{vmatrix} \frac{-d \cos \theta}{\tau^2} & \frac{-d \sin \theta}{\tau} \\ 0 & 1 \end{vmatrix} \\
 &= \frac{-d \cos \theta}{\tau^2} .
 \end{aligned}$$

The probability density function for the time lag τ is

$$p(\tau) = \frac{dF(\tau)}{d\tau} = \frac{1}{|\tau|} \frac{d}{d\tau} \int_{-\pi}^{\pi} p(V, \theta) \cos \theta d\theta .$$

For bivariate polynomial probability densities

$$\begin{aligned}
 p(V, \theta) &= \sum_{i=0}^M \sum_{j=0}^N a_{ij} V^i \theta^j \\
 &= \sum_{i=0}^M \sum_{j=0}^N a_{ij} \left(\frac{d \cos \theta}{\tau} \right)^i \theta^j ,
 \end{aligned}$$

the integrand is of the form

$$\sum_{i=0}^M \sum_{j=0}^N b_{ij} (\cos \theta)^{i+1} \theta^j$$

and can be evaluated analytically.

B. UNIFORM RECTANGULAR DISTRIBUTION

In this model, the probability density is uniform over a rectangle in velocity-azimuth space:

$$p(V, \theta) = \begin{cases} \frac{1}{(V_{\max} - V_{\min})(\theta_{\max} - \theta_{\min})} & \text{if } V_{\min} < V < V_{\max} \\ & \text{and } \theta_{\min} < \theta < \theta_{\max} \\ 0 & \text{otherwise.} \end{cases}$$

The time-lag probability density function is

$$\begin{aligned} p(\tau) &= \frac{d}{|\tau|(V_{\max} - V_{\min})(\theta_{\max} - \theta_{\min})} \int_{\theta(\tau)} \cos \theta \, d\theta \\ &= \frac{d \sin \theta}{|\tau|(V_{\max} - V_{\min})(\theta_{\max} - \theta_{\min})} \Big|_{\theta(\tau)} \end{aligned}$$

If the shaded areas above θ_{\max} and below θ_{\min} in Figure V-1 are removed, then the remaining shaded area determines the limits of integration for θ at any particular time lag τ . Since the angles θ along the curved boundaries in Figure V-1 are of the form $\cos^{-1}(V\tau/d)$ and $-\cos^{-1}(V\tau/d)$, the following identities are useful in the integral evaluation:

$$\sin \left[\cos^{-1} \left(\frac{V\tau}{d} \right) \right] = \sqrt{1 - \left(\frac{V\tau}{d} \right)^2}$$

$$\sin \left[-\cos^{-1} \left(\frac{V\tau}{d} \right) \right] = - \sqrt{1 - \left(\frac{V\tau}{d} \right)^2} .$$

As in the case of the Section III sector-of-annulus model, subdividing the angular range $\theta_{\min} < \theta < \theta_{\max}$ into sections bounded by the multiple-of- π transition angles encountered as θ progresses from θ_{\min} to θ_{\max} facilitates the determination of $p(\tau)$. As before, sections can be mapped into the first and second quadrants so that the probability density as a function of τ is unaffected. The same procedure outlined in Figure III-4 is also sufficient to ascertain the minimum angle α and the maximum angle β of each section after mapping onto the first and second quadrants. Addition of the contributions from the appropriate sections at the time lag τ again determines the probability density function $p(\tau)$. If θ_{\min} and θ_{\max} are specified so that $-2\pi \leq \theta_{\min} < 2\pi$, $-2\pi < \theta_{\max} \leq 2\pi$, and $\theta_{\min} < \theta_{\max} \leq \theta_{\min} + 2\pi$, then there are no more than three such sections.

The extremal values of θ for any particular time lag τ lie either on horizontal section boundaries or on arc-cosine curves. The boundaries in the rectangular velocity-azimuth model correspond precisely to the boundaries of the inverse-velocity sector-of-annulus model in Section III. The difference between the two models is the probability density within the boundaries: if the uniform rectangular velocity-azimuth model were expressed in terms of the inverse velocity model, the probability density would rise as the vector magnitude $|\vec{u}|$ decreases. As in the case of the sector-of-annulus model, there are, for any give pair of angles α and β , three possible τ intervals where the formula for $p(\tau)$ is different. In the first and last of these intervals, one extremal value of θ is on a horizontal section boundary, while the other is on an arc-cosine curve. In the middle interval, both extremal values lie either on arc-cosine curves or on horizontal section boundaries.

If $\pi/2 < \beta$, then the first interval is $(d \cos \beta / V_{\min}) \leq \tau \leq \min [(d \cos \beta / V_{\max}), (d \cos \alpha / V_{\min})]$ and

$$p(\tau) = \frac{d \left\{ \sin \beta - \sin \left[\cos^{-1} \left(\frac{V_{\min} \tau}{d} \right) \right] \right\}}{|\tau| \tau (V_{\max} - V_{\min}) (\theta_{\max} - \theta_{\min})}$$

$$= \frac{\sqrt{d^2 - (V_{\min} \tau)^2} - d \sin \beta}{\tau^2 (V_{\max} - V_{\min}) (\theta_{\max} - \theta_{\min})}$$

If $\beta < \pi/2$, then the first interval is $(d \cos \beta / V_{\max}) \leq \tau \leq \min [(d \cos \beta / V_{\min}), (d \cos \alpha / V_{\max})]$ and

$$p(\tau) = \frac{d \left\{ \sin \beta - \sin \left[\cos^{-1} \left(\frac{V_{\max} \tau}{d} \right) \right] \right\}}{\tau^2 (V_{\max} - V_{\min}) (\theta_{\max} - \theta_{\min})}$$

$$= \frac{d \sin \beta - \sqrt{d^2 - (V_{\max} \tau)^2}}{\tau^2 (V_{\max} - V_{\min}) (\theta_{\max} - \theta_{\min})}$$

If $\beta = \pi/2$, the first interval is of zero length, and the formula for the second interval should be used at $\tau = 0$.

If $\max [(d \cos \beta / V_{\min}), (d \cos \beta / V_{\max})] \leq \tau \leq \min [(d \cos \alpha / V_{\min}), (d \cos \alpha / V_{\max})]$, then the extremal values of θ in the second interval are on arc-cosine curves and

$$\begin{aligned}
p(\tau) &= \frac{d \left\{ \sin \left[\cos^{-1} \left(\frac{V_{\min} \tau}{d} \right) \right] - \sin \left[\cos^{-1} \left(\frac{V_{\max} \tau}{d} \right) \right] \right\}}{\tau^2 (V_{\max} - V_{\min})(\theta_{\max} - \theta_{\min})} \\
&= \frac{\sqrt{d^2 - (V_{\min} \tau)^2} - \sqrt{d^2 - (V_{\max} \tau)^2}}{\tau^2 (V_{\max} - V_{\min})(\theta_{\max} - \theta_{\min})} \\
&= \frac{V_{\min} + V_{\max}}{(\theta_{\max} - \theta_{\min}) \left[\sqrt{d^2 - (V_{\min} \tau)^2} + \sqrt{d^2 - (V_{\max} \tau)^2} \right]}
\end{aligned}$$

If $\min \left[(d \cos \alpha / V_{\min}), (d \cos \alpha / V_{\max}) \right] \leq \tau \leq \max \left[(d \cos \beta / V_{\min}), (d \cos \beta / V_{\max}) \right]$, then the extremal values of θ are on horizontal section boundaries and

$$p(\tau) = \frac{d |\sin \beta - \sin \alpha|}{\tau^2 (V_{\max} - V_{\min})(\theta_{\max} - \theta_{\min})}$$

If the limits for the second interval are equal, then only the formulas for the first and third intervals should be used.

If $\pi/2 < \alpha$, then the third interval is $\max \left[(d \cos \beta / V_{\max}), (d \cos \alpha / V_{\min}) \right] \leq \tau \leq (d \cos \alpha / V_{\max})$ and

$$\begin{aligned}
p(\tau) &= \frac{d \left\{ \sin \left[\cos^{-1} \left(\frac{V_{\max} \tau}{d} \right) \right] - \sin \alpha \right\}}{|\tau| \tau (V_{\max} - V_{\min})(\theta_{\max} - \theta_{\min})} \\
&= \frac{d \sin \alpha - \sqrt{d^2 - (V_{\max} \tau)^2}}{\tau^2 (V_{\max} - V_{\min})(\theta_{\max} - \theta_{\min})}
\end{aligned}$$

If $\alpha < \pi/2$, then the third interval is

$\max [(d \cos \beta / V_{\min}), (d \cos \alpha / V_{\max})] \leq \tau \leq (d \cos \alpha / V_{\min})$ and

$$p(\tau) = \frac{d \left\{ \sin \left[\cos^{-1} \left(\frac{V_{\min} \tau}{d} \right) \right] - \sin \alpha \right\}}{\tau^2 (V_{\max} - V_{\min})(\theta_{\max} - \theta_{\min})}$$

$$= \frac{\sqrt{d^2 - (V_{\min} \tau)^2} - d \sin \alpha}{\tau^2 (V_{\max} - V_{\min})(\theta_{\max} - \theta_{\min})}$$

If $\alpha = \pi/2$, the third interval is of zero length, and the formula for the second interval should be used at $\tau = 0$.

Figures V-2 and V-3 present, for the uniform rectangular velocity-azimuth distribution, the time-lag probability density function $p(\tau)$ at $V_{\min}/V_{\max} = 0.1$ and $V_{\min}/V_{\max} = 0.9$, respectively, for various 30° sectors. At $V_{\min}/V_{\max} = 0.1$, there are sharp peaks near $\tau = 0$ in Figure V-2 (in sharp contrast to the corresponding inverse velocity model of Figure III-6). At $V_{\min}/V_{\max} = 0.9$, however, there is a strong resemblance in Figure V-3 to the comparable inverse velocity model time-lag probability density functions in Figure III-7.

$$\theta_{\min} = -10^\circ$$

$$\theta_{\max} = 20^\circ$$

$$p(\tau) = \frac{2V_{\min}}{\pi d}$$

$$\tau = \frac{-d}{V_{\min}} \qquad \tau = \frac{d}{V_{\min}}$$

$$\theta_{\min} = 62^\circ$$

$$\theta_{\max} = 92^\circ$$

$$\theta_{\min} = 278^\circ$$

$$\theta_{\max} = 308^\circ$$

$$p(\tau) = \frac{2V_{\min}}{\pi d}$$

$$\tau = \frac{-d}{V_{\min}} \qquad \tau = \frac{d}{V_{\min}}$$

$$p(\tau)$$

$$\theta_{\min} = 134^\circ$$

$$\theta_{\max} = 164^\circ$$

$$p(\tau)$$

$$\theta_{\min} = 206^\circ$$

$$\theta_{\max} = 236^\circ$$

FIGURE V-2

TIME-LAG PROBABILITY DENSITY FUNCTION FOR THE UNIFORM RECTANGULAR VELOCITY-AZIMUTH MODEL AT $V_{\min}/V_{\max} = 0.1$ FOR VARIOUS 30° SECTORS

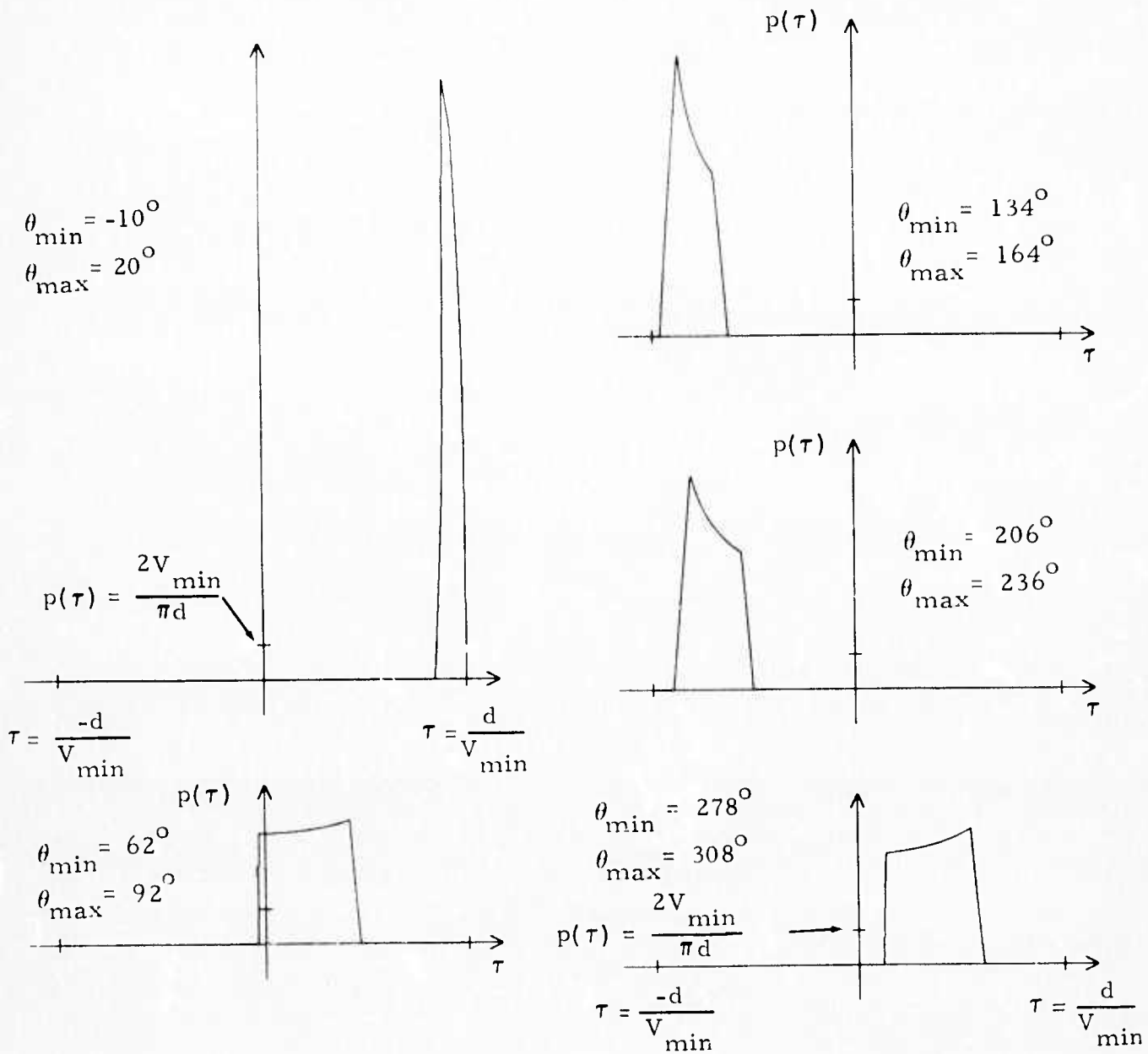


FIGURE V-3

TIME-LAG PROBABILITY DENSITY FUNCTION FOR THE UNIFORM
 RECTANGULAR VELOCITY-AZIMUTH MODEL AT
 $V_{\min}/V_{\max} = 0.9$ FOR VARIOUS 30° SECTORS

C. TAPERED-VELOCITY UNIFORM-AZIMUTH DISTRIBUTION

In this model, the probability density is nonzero within a rectangle in velocity-azimuth space and is the product of the velocity probability density function $p(V)$ and the arrival angle probability density function $p(\theta)$:

$$p(V, \theta) = p(V) p(\theta) .$$

The velocity probability density function $p(V)$ is smooth and falls off to zero at the minimum and maximum velocities. It is specified over three equally long intervals by quadratic functions. In the first interval, where

$$V_{\min} \leq V \leq (2V_{\min} + V_{\max})/3,$$

$$p(V) = \frac{27(V - V_{\min})^2}{2(V_{\max} - V_{\min})^3} .$$

In the second interval, in which $(2V_{\min} + V_{\max})/3 \leq V \leq (V_{\min} + 2V_{\max})/3$,

$$p(V) = \frac{9}{4(V_{\max} - V_{\min})} - \frac{27(V - V_{\text{med}})^2}{(V_{\max} - V_{\min})^2} ,$$

where $V_{\text{med}} = (V_{\min} + V_{\max})/2$ is the mean velocity. In the third interval, where $(V_{\min} + 2V_{\max})/3 \leq V \leq V_{\max}$,

$$p(V) = \frac{27(V_{\max} - V)^2}{2(V_{\max} - V_{\min})^3} .$$

Figure V-4 shows the velocity probability density function $p(V)$. If V_a and V_b designate the minimum and maximum velocity, respectively, for the i -th interval, then

$$V_a = \frac{(3-i) V_{\min} + i V_{\max}}{3}$$

and

$$V_b = \frac{(4-i) V_{\min} + (i-1) V_{\max}}{3} .$$

The arrival-angle probability density function $p(\theta)$ is uniform between θ_{\min} and θ_{\max} :

$$p(\theta) = \begin{cases} \frac{1}{\theta_{\max} - \theta_{\min}} & \text{if } \theta_{\min} < \theta < \theta_{\max} \\ 0 & \text{otherwise.} \end{cases}$$

As in earlier models, breaking up the angular range $\theta_{\min} < \theta < \theta_{\max}$ into sections in accordance with the procedure depicted in Figure III-4 and subsequently adding the contributions from the appropriate sections can simplify determination of the time-lag probability density function $p(\tau)$. As before, α and β denote the minimum angle and the maximum angle, respectively, of each section after mapping onto the first and second quadrant. At the time lag τ , the contribution to $p(\tau)$ from each section is

$$\frac{1}{|\tau|} \frac{d}{d\tau} \int_{\omega_{\min}}^{\omega_{\max}} p(V, \theta) \cos \theta d\theta ,$$

where ω_{\min} and ω_{\max} are the minimum and maximum angles, respectively, at the time lag τ after the rectangle described by $\alpha \leq \theta \leq \beta$ and $V_{\min} \leq V \leq V_{\max}$ is transformed into (τ, θ) space. The term $|\tau|$ in the denominator may be replaced by τ if the integration limits are reversed when τ is negative.

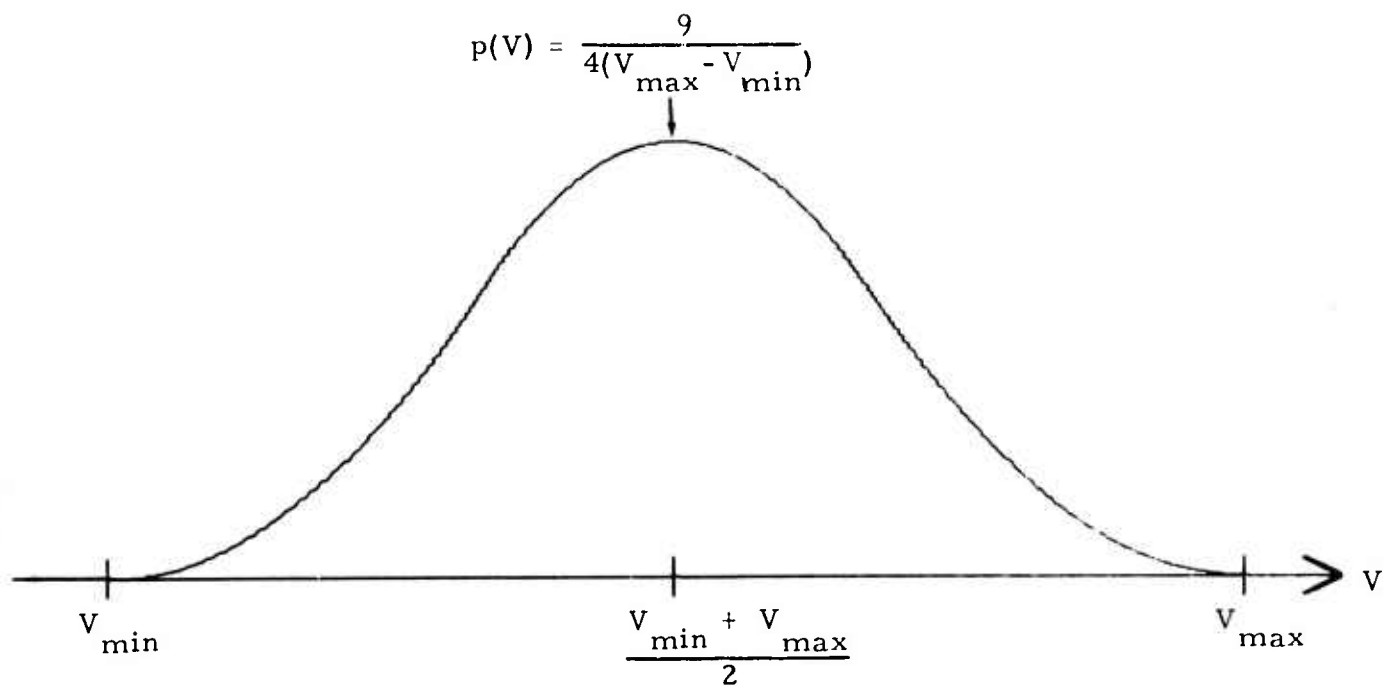


FIGURE V-4
TAPERED VELOCITY PROBABILITY DENSITY FUNCTION

The contributions from each velocity interval at the time lag τ must be determined separately and summed to obtain the contribution from each sector. In this process, integrals of the form

$$\begin{aligned} \int (V - V_o)^2 \cos \theta d\theta &= \int \left(\frac{d \cos \theta}{\tau} - V_o \right)^2 \cos \theta d\theta \\ &= \frac{d^2}{\tau^2} \left[\frac{1}{3} \sin \theta (\cos^2 \theta + 2) \right] \\ &\quad - \frac{2V_o d}{\tau} \left[\frac{1}{2} \sin \theta \cos \theta + \frac{1}{2} \theta \right] + V_o^2 \sin \theta \\ &= \frac{d^2}{\tau^2} \left\{ \sin \theta \left[\frac{1}{3} \cos^2 \theta - \left(\frac{V_o \tau}{d} \right) \cos \theta \right. \right. \\ &\quad \left. \left. + \left(\frac{V_o \tau}{d} \right)^2 + \frac{2}{3} \right] - \left(\frac{V_o \tau}{d} \right) \theta \right\} \end{aligned}$$

occur for each velocity interval.

The contribution to $p(\tau)$ is

$$\begin{aligned} &\frac{27 d^3}{2(V_{\max} - V_{\min})^3 (\theta_{\max} - \theta_{\min}) \tau^4} \left\{ \sin \theta \left[\frac{1}{3} \cos^2 \theta \right. \right. \\ &\quad \left. \left. - \left(\frac{V_{\min} \tau}{d} \right) \cos \theta + \left(\frac{V_{\min} \tau}{d} \right)^2 + \frac{2}{3} \right] - \left(\frac{V_{\min} \tau}{d} \right) \theta \right\} \Bigg|_{\theta_b}^{\theta_a} \end{aligned}$$

in the first velocity interval,

$$\frac{9d \sin \theta}{4(V_{\max} - V_{\min})(\theta_{\max} - \theta_{\min}) \tau^2} \Bigg|_{\theta_a}^{\theta_b}$$

$$- \frac{27d^3}{(V_{\max} - V_{\min})^3 (\theta_{\max} - \theta_{\min}) \tau^4} \left\{ \sin \theta \left[\frac{1}{3} \cos^2 \theta \right. \right.$$

$$\left. \left. - \left(\frac{V_{\text{med}} \tau}{d} \right) \cos \theta + \left(\frac{V_{\text{med}} \tau}{d} \right)^2 + \frac{2}{3} \right] - \left(\frac{V_{\text{med}} \tau}{d} \right) \theta \right\} \Bigg|_{\theta_a}^{\theta_b}$$

in the second velocity interval, and

$$\frac{27d^3}{2(V_{\max} - V_{\min})^3 (\theta_{\max} - \theta_{\min}) \tau^4} \left\{ \sin \theta \left[\frac{1}{3} \cos^2 \theta \right. \right.$$

$$\left. \left. - \left(\frac{V_{\max} \tau}{d} \right) \cos \theta + \left(\frac{V_{\max} \tau}{d} \right)^2 + \frac{2}{3} \right] - \left(\frac{V_{\max} \tau}{d} \right) \theta \right\} \Bigg|_{\theta_a}^{\theta_b}$$

in the third velocity interval, where θ_a and θ_b are yet to be specified.

In the discussion which follows, V_a is the minimum velocity of the i -th velocity interval and V_b the maximum velocity. If $\pi/2 < \alpha < \beta$, there is a contribution to $p(\tau)$ when $(d \cos \beta / V_a) < \tau < (d \cos \alpha / V_b)$. In this case, the upper integration limit is

$$\theta_b = \cos^{-1} \left(\frac{V_a \tau}{d} \right)$$

when $(d \cos \beta / V_a) < \tau \leq (d \cos \alpha / V_a)$ or $\theta_b = \alpha$ when $(d \cos \alpha / V_a) < \tau < (d \cos \alpha / V_b)$. The lower integration limit is $\theta_a = \beta$ when $(d \cos \beta / V_a) < \tau < (d \cos \beta / V_b)$ or

$$\theta_a = \cos^{-1} \left(\frac{V_b \tau}{d} \right)$$

when $(d \cos \beta / V_b) \leq \tau < (d \cos \alpha / V_b)$.

If $\alpha < \beta < \pi/2$, there is a contribution to $p(\tau)$ when $(d \cos \beta / V_b) < \tau < (d \cos \alpha / V_a)$. In this case, the upper integration limit is $\theta_b = \beta$ when $(d \cos \beta / V_b) < \tau < (d \cos \beta / V_a)$ or

$$\theta_b = \cos^{-1} \left(\frac{V_a \tau}{d} \right)$$

when $(d \cos \beta / V_a) \leq \tau < (d \cos \alpha / V_a)$. The lower integration limit is

$$\theta_a = \cos^{-1} \left(\frac{V_b \tau}{d} \right)$$

when $(d \cos \beta / V_b) < \tau \leq (d \cos \alpha / V_b)$ or $\theta_a = \alpha$ when $(d \cos \alpha / V_b) < \tau < (d \cos \alpha / V_a)$.

If $\alpha \leq \pi/2 < \beta$, there is a contribution to $p(\tau)$ when $(d \cos \beta / V_a) < \tau < (d \cos \alpha / V_a)$ and the upper integration limit is always

$$\theta_b = \cos^{-1} \left(\frac{V_a \tau}{d} \right) .$$

The lower integration limit is $\theta_a = \beta$ when $(d \cos \beta / V_a) < \tau < (d \cos \beta / V_b)$ or

$$\theta_a = \cos^{-1} \left(\frac{V_b \tau}{d} \right)$$

when $(d \cos \beta / V_b) \leq \tau \leq (d \cos \alpha / V_b)$ or $\theta_a = \alpha$ when $(d \cos \alpha / V_b) < \tau < (d \cos \alpha / V_a)$.

If $\alpha \leq \pi/2 \leq \beta$ and $\tau = 0$, there is no simple method to eliminate the powers of τ in the denominator of the integrals to be evaluated. However, the probability $P(0 \leq \tau_o \leq \tau)$ that τ_o lies between 0 and τ is

$$\begin{aligned} & \int_{V_{\min}}^{V_{\max}} p(V) \left[\int_{\cos^{-1}\left(\frac{V\tau}{d}\right)}^{\frac{\pi}{2}} p(\theta) d\theta \right] dV \\ &= \int_{V_{\min}}^{V_{\max}} p(V) \left[\int_{\frac{\pi}{2} - \sin^{-1}\left(\frac{V\tau}{d}\right)}^{\frac{\pi}{2}} p(\theta) d\theta \right] dV \\ &= \frac{1}{\theta_{\max} - \theta_{\min}} \int_{V_{\min}}^{V_{\max}} p(V) \sin^{-1}\left(\frac{V\tau}{d}\right) dV \end{aligned}$$

when τ is small enough, and the probability density function $p(\tau)$ is

$$\begin{aligned} \frac{dP(0 \leq \tau_o \leq \tau)}{d\tau} &= \frac{1}{\theta_{\max} - \theta_{\min}} \int_{V_{\min}}^{V_{\max}} \frac{d}{d\tau} \left[\sin^{-1}\left(\frac{V\tau}{d}\right) \right] p(V) dV \\ &= \frac{1}{d(\theta_{\max} - \theta_{\min})} \int_{V_{\min}}^{V_{\max}} \frac{p(V) V dV}{\sqrt{1 - \left(\frac{V\tau}{d}\right)^2}} \end{aligned}$$

At $\tau = 0$,

$$\begin{aligned}
 p(\tau) &= \frac{1}{d(\theta_{\max} - \theta_{\min})} \int_{V_{\min}}^{V_{\max}} p(V) V dV \\
 &= \frac{V_{\min} + V_{\max}}{2d(\theta_{\max} - \theta_{\min})}
 \end{aligned}$$

since the integral expression is simply the average velocity for a velocity probability density function symmetrical about $(V_{\min} + V_{\max})/2$.

For the tapered-velocity uniform-azimuth distribution, Figures V-5 and V-6 depict the time-lag probability density function $p(\tau)$ at $V_{\min}/V_{\max} = 0.1$ and $V_{\min}/V_{\max} = 0.9$, respectively, for specified 30° sectors. In this particular model, the functions $p(\tau)$ are smooth and continuous unless

θ_{\min} or θ_{\max} is an odd integer multiple of $\pi/2$. The probability density functions $p(\tau)$ in Figure V-6 resemble those of Figure III-7, IV-2, and V-3: when the minimum and maximum velocities are nearly equal, the dominant influence on $p(\tau)$ is apparently the specific angular range $\theta_{\min} < \theta < \theta_{\max}$ of the uniform azimuthal distribution.

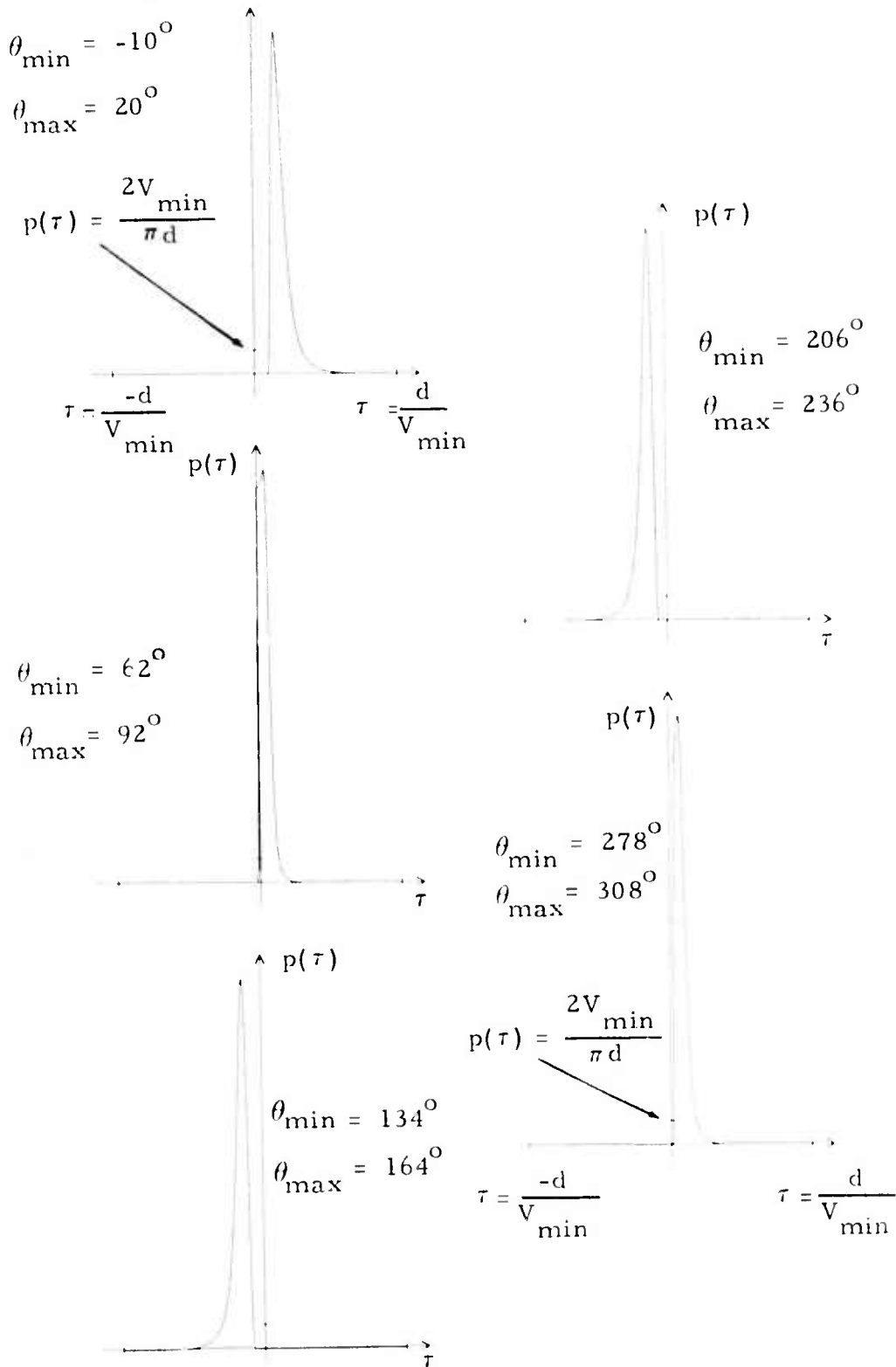


FIGURE V-5

TIME-LAG PROBABILITY DENSITY FUNCTION FOR THE TAPERED-VELOCITY UNIFORM-AZIMUTH MODEL AT $V_{\min}/V_{\max} = 0.1$ FOR VARIOUS 30° SECTORS

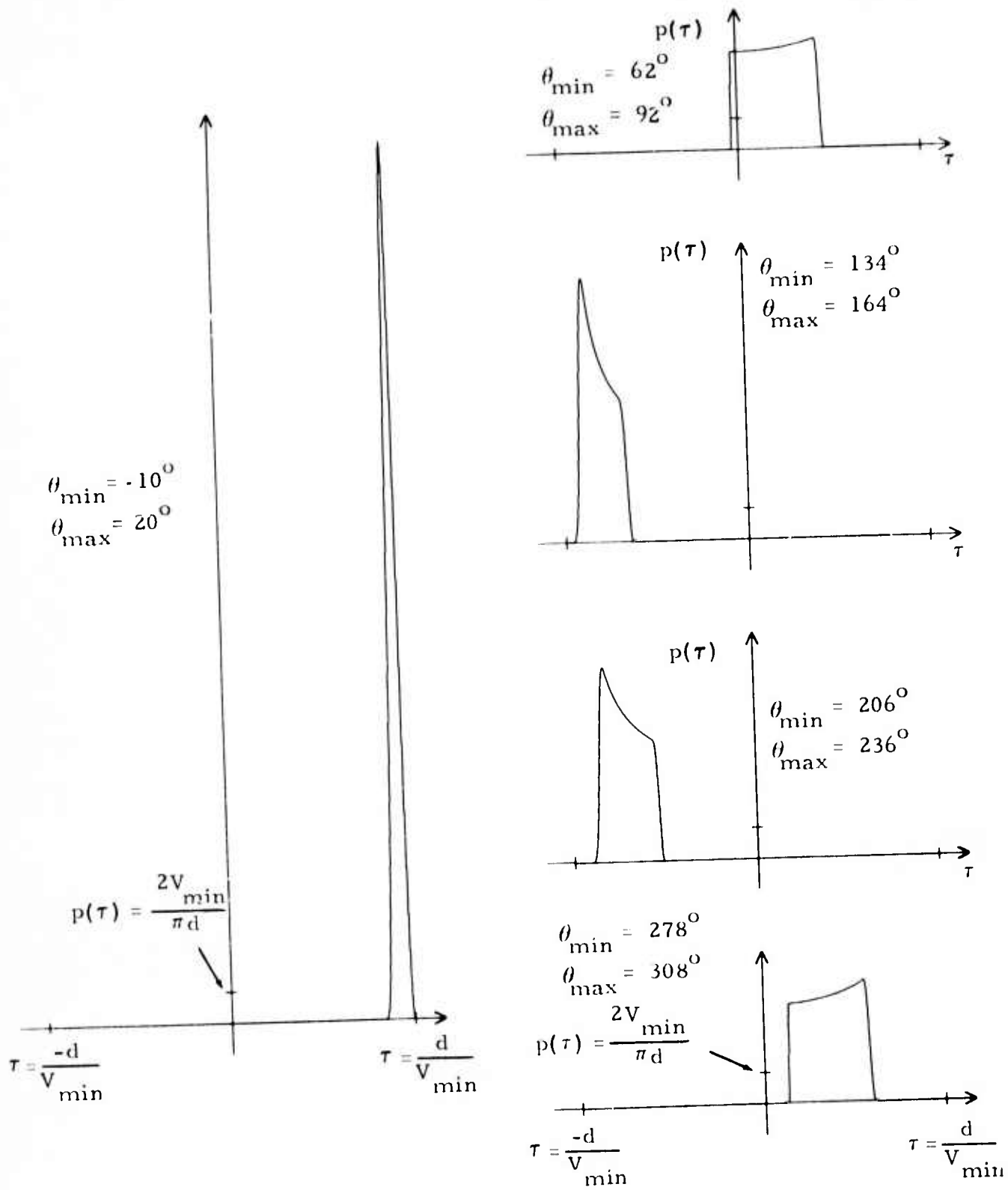


FIGURE V-6

TIME-LAG PROBABILITY DENSITY FUNCTION FOR THE TAPERED-VELOCITY UNIFORM-AZIMUTH MODEL AT $V_{\min}/V_{\max} = 0.9$ FOR VARIOUS 30° SECTORS

SECTION VI

SUMMARY

This report has presented two algorithms for implementing Wiener adaptive multichannel filtering with distributed signal models. These algorithms may prove useful in eliminating or ameliorating problems previously encountered with maximum likelihood adaptive multichannel filtering. Among these problems are mutual cancellation of interfering events, signal distortion, and sensitivity to slight deviations from an ideal plane-wave signal model. The two algorithms discussed require some method for estimating the crosscorrelation functions between the signal and the channels entering the adaptive beamformer. These crosscorrelation functions are estimated by convolving the time-lag probability density function $p(\tau)$ corresponding to a specified velocity-azimuth incoming-energy distribution with the signal autocorrelation function, which is approximated by averaging the input-channel autocorrelation functions.

Estimating the time-lag probability density function $p(\tau)$ for various directionally-distributed signal models is an interesting problem in its own right. In this report, three basic models are described. The first is an inverse velocity space model, in which the signal-model probability distributions are specified as a function of the two-dimensional inverse velocity vector $\vec{u} = \vec{V}/(\vec{V} \cdot \vec{V})$, where \vec{V} is the incoming energy's apparent velocity in the plane of the array. The second is a distributed ring model where all incoming energy is concentrated at a single apparent velocity V with respect to the plane of the array, but is distributed over a range of azimuths according to a known probability density function $p_{\theta}(\theta)$. The final model is a velocity-azimuth space model, in which the signal model is specified both as a function of the apparent velocity V in the plane of the array and as a function of the arrival azimuth θ .

SECTION VII
REFERENCE

Barnard, Thomas E., and Leo J. O'Brien, 31 December 1974, "An Evaluation of Adaptive-Beamforming Techniques Applied to Recorded Seismic Data," Technical Report No. 8, VELA Network Evaluation and Automatic Processing Research, Texas Instruments Incorporated.